Sara Filipa Correia de Brito

Licenciatura em Bioquímica

Therapeutic rescue of NPC phenotype by CYP46A1 cerebellar expression

Dissertação para obtenção do Grau de Mestre em
Genética Molecular e Biomedicina

Orientadora: Doutora Elsa Rodrigues, Professora Associada, Faculdade de Farmácia da Universidade de Lisboa

Co-orientadora: Doutora Margarida Castro-Caldas Braga, Professora Auxiliar, Faculdade de Ciências e Tecnologia da Universidade Nova de Lisboa

Júri:

Presidente: Prof. Doutora Paula Maria Theriaga Mendes Bernardes Gonçalves, Professora Associada da Faculdade de Ciências e Tecnologia da Universidade Nova de Lisboa

Arguente: Prof. Doutora Sara Alves Xapelli, Professora Auxiliar da Faculdade de Medicina da Universidade de Lisboa

Vogal: Prof. Doutora Elsa Rodrigues, Professora Associada da Faculdade de Farmácia da Universidade de Lisboa

FACULDADE DE CIÊNCIAS E TECNOLOGIA
UNIVERSIDADE NOVA DE LISBOA

Novembro 2020

Sara Filipa Correia de Brito

Licenciatura em Bioquímica

Therapeutic rescue of NPC phenotype by CYP46A1 cerebellar expression

Dissertação para obtenção do Grau de Mestre em
Genética Molecular e Biomedicina

Orientadora: Doutora Elsa Rodrigues, Professora Associada, Faculdade de Farmácia da Universidade de Lisboa

Co-orientadora: Doutora Margarida Castro-Caldas Braga, Professora Auxiliar, Faculdade de Ciências e Tecnologia da Universidade Nova de Lisboa

Novembro 2020

“Therapeutic rescue of NPC phenotype by CYP46A1 cerebellar expression”

This work was supported by FEDER and national funds from Fundação para a Ciência e Tecnologia (FCT) (LISBOA-01-0145-FEDER/030104; PTDC/MED-NEU/29455/2017).

Agradecimentos

Em primeiro lugar, gostaria de agradecer à minha família, por todo o apoio que me têm dado sempre.

Quero agradecer às prof. Elsa e Margarida, por me terem dado a oportunidade de trabalhar neste projeto e por todo o apoio prestado e disponibilidade.

Por último, quero agradecer a toda a gente no laboratório, prof. Maria João Gama, Andreia, Maria, Viviana, Rita, Daniela por toda a disponibilidade e simpatia.

Resumo

A doença de Niemann-Pick de tipo C (NPC) é uma doença neurodegenerativa caracterizada pela acumulação de colesterol e outros lípidos nos endossomas tardios/ lisossomas, com opções terapêuticas limitadas. Assim, existe um elevado interesse no desenvolvimento de estratégias terapêuticas para esta doença. Neste trabalho, foi utilizada terapia genética mediada por um vetor AAV que codifica para CYP46A1, o enzima responsável pela principal via de eliminação do colesterol no encéfalo, resultando no aumento da expressão desta proteína. O vetor foi injetado em ratinhos Npc1$^{tm(I1061T)}$, que têm um *knock-in* da mutação NPC1I1061T, a mais comum em pacientes de NPC.

A expressão de CYP46A1 levou a um incremento positivo do ganho de peso nas fêmeas nos últimos estadios da doença, não tendo sido o mesmo observado nos machos, o que provavelmente se deve à heterogeneidade fenotípica observada nos animais Npc1$^{tm(I1061T)}$. O aumento de expressão do CYP46A1, não conseguiu prevenir significativamente a extensa perda de neurónios de Purkinje no cerebelo, nem melhorou a função motora, avaliada pelo teste do rotarod e pela avaliação funcional da marcha. No entanto, a análise molecular e bioquímica sugere que a expressão ectópica do CYP46A1 melhora características importantes da doença, tais como a homeostasia do colesterol, a função lisossomal e a neuroinflamação. De facto, nos murganhos injetados com o vetor AAV-CYP46A1, podemos ver uma restauração dos níveis de mRNA da 3-hidroxi-3-metilglutaril-coenzima A redutase e da catepsina D, juntamente com a redução na acumulação da forma lipidada da proteína LC3-II, indicando recuperação da homeostase do colesterol e uma melhoria do tráfego intracelular. Além disso, o CYP6A1 diminui a astrogliose e a microgliose no cerebelo de machos NPC. No seu conjunto, os nossos resultados são promissores e sugerem que uma intervenção precoce poderá eventualmente abrir uma nova via terapêutica para esta doença.

Palavras-chave: Doença de Niemann-Pick de tipo C (NPC), CYP46A1, colesterol, células de Purkinje, neuroinflamação, função motora

Abstract

Niemann-Pick type C (NPC) disease is a rare neurogenerative disorder characterized by accumulation of cholesterol and other lipids in late endosomes/lysosomes. There are still limited therapeutic options available for NPC, but as it causes motor and intellectual impairment and premature death there is a high interest in the development of therapeutic strategies for this disease. CYP46A1 is a key enzyme involved in cholesterol homeostasis, which converts cholesterol to 24 (S)-hydroxycholesterol, being responsible for half of cholesterol turnover and the major brain cholesterol elimination pathway. Interestingly, increasing the expression or activity of the CYP46A1 resulted in beneficial effects in several animal models for neurodegenerative diseases. In this work, we aimed to study whether increased CYP46A1 expression would improve disease-associated biochemical alterations and disease phenotype in $Npc1^{tm(I1061T)}$ mice, that have a knock-in of the NPC1I1061T mutation, the most common mutation in NPC patients. For that, we used adeno-associated virus gene mediated therapy with a vector encoding CYP46A1, resulting in CYP46A1 ectopic expression.

Increased expression of CYP46A1 led to a positive increment in weight gain in female mice in later stages of the disease, nevertheless the same was not observed in males, probably because of the phenotypic heterogeneity observed between $Npc1^{tm(I1061T)}$ animals. CYP46A1 expression could not significantly prevent extensive Purkinje cell loss in the cerebellum, nor it ameliorated motor function, as assessed by the rotarod test and gait analysis. Nevertheless, molecular and biochemical analysis suggest that CYP46A1 ectopic expression is able to ameliorate important features of NPC disease, such as cholesterol homeostasis, lysosomal function and neuroinflammation. Indeed, CYP46A1 restores 3-hydroxy-3-methylglutaryl-coenzyme A reductase and cathepsin D mRNA levels, together with reduction in the accumulation of lipidated microtubule-associated protein 1A/1B light chain 3B (LC3-II) indicating restoration of cholesterol homeostasis and improvement of the cellular intracellular traffic. Moreover, CYP46A1 expression could decrease astrogliosis and microgliosis in NPC male mice cerebellum. Overall, our promising results suggest that an earlier intervention, before the onset of the disease, can eventually open a new therapeutic avenue for this disease.

Keywords: Niemann-Pick type C (NPC) disease, CYP46A1, cholesterol, Purkinje cells, neuroinflammation, motor function

Table of Contents

List of Figures

List of Tables

List of Abbreviations

24OHC- 24 (S)-hydroxycholesterol

Aß- Amyloid-ß

AAV- Adeno-associated virus

ABCA1- ATP binding cassette transporter A1

ACAT1- Acetyl-CoA acetyltransferase 1

AD- Alzheimer's disease

AP-1- Activator protein-1

Apoe- Apolipoprotein E

BBB- Blood-brain-barrier

Ccl2- C-C motif chemokine 2

CD11b- Cluster of Differentiation 11b

CD45- Cluster of Differentiation 45

CD68- Cluster of Differentiation 68

CNS- Central nervous system

CtsD- Cathepsin D

Cx3cr1- Chemokine (C-X3-C motif) receptor 1

Cxcl10- C-X-C motif chemokine 10

CYP46A1- Cholesterol 24-hydroxylase

EDTA- Ethylenediaminetetraacetic acid

EGTA- Ethylene glycol tetraacetic acid

ER- Endoplasmic reticulum

FDA- Food and Drug Administration

GAPDH- Glyceraldehyde 3-phosphate dehydrogenase

GFAP- Glial fibrillary acidic protein

GFP- Green fluorescent protein

GPCRs- G protein-coupled receptors

H3K27ac- Acetylation of histone H3 on lysine 27

H3K4me2- Histone H3 lysine 4 dimethylation

HD- Huntington's disease

HDAC- Histone deacetylase

HMG-CoA- 3-hydroxy-3-methylglutaryl-CoA

HMGR- HMG-CoA reductase

HMGS- HMG-CoA synthase

HP- β- CD- 2-hydroxypropyl-beta-cyclodextrin

HRP- Horseradish peroxidase

Iba-1- Ionized calcium-binding adapter molecule 1

IDOL- Inducible degrader of LDLR

IκB-α- Inhibitor of nuclear factor kappa B alpha

IKKβ- Inhibitor of nuclear factor kappa-B kinase subunit beta

IL-1α- Interleukin-1α

IL-1β- Interleukin-1β

INSIG- Insulin induced gene

Irf1- Interferon regulatory factor 1

LC-3- Microtubule-associated protein 1A/1B-light chain 3B

LDL- Low density lipoprotein

LDLR- Low density lipoprotein receptor

LXR- Liver X Receptors

mRNA- Messenger RNA

NF-κB- Nuclear factor kappa B

NMDARs- N-methyl-D-aspartate receptors

NPC- Niemann-Pick type C

NPC1- Niemann–Pick C1 protein

NPC2- Niemann-Pick type C2 protein

P2ry12/13- Purinergic receptor P2Y, G-protein coupled 12/13

PCR- Polymerase chain reaction

PD- Parkinson's disease

PFA- Paraformaldehyde

Pu.1- Spi-1 proto-oncogene

RNA- Ribonucleic acid

RT- qPCR- Quantitative Real-Time PCR

Sall1- Spalt like transcription factor 1

SCA3- Spinocerebellar Ataxia 3

SCAP- SREBP cleavage-activating protein

SDS- Sodium dodecyl sulphate

SEM- Standard error of mean

sGTPases- Small guanosine triphosphate-binding proteins

SLOS- Smith**-** Lemli Opitz syndrome

SNARE- Soluble N-ethylmaleimide-sensitive factor attachment protein receptors

SREBP-2- Sterol regulatory- element binding protein 2

SUMO- Small Ubiquitin-like Modifier

TBS-T- Tris-buffered saline-tween

Tg- Transgenic

Tmem119- Transmembrane protein 119

TNF-α- Tumor necrosis factor α

Trem2- Triggering receptor expressed on myeloid cells 2

WT- Wild type

1. Introduction

1.1. Brain cholesterol and its role in neurodegeneration

Cholesterol is an amphipathic sterol, being an important component of the membrane bilayers, playing structural and physiological roles through regulation of various signaling pathways in mammalian cells [1, 2]. Cholesterol is necessary for production of steroid hormones and bile acids, the fluidity and permeability of cell membranes, the composition of lipid rafts, which are involved in various aspects of neuronal function, including growth factor signaling, axon guidance and synaptic transmission [3, 4]**.** Due to its fundamental role in neuronal biology, it is expected that alterations in the levels of cholesterol in the brain may result in neurodegeneration [2].

The brain contains about 25% of the total cholesterol of the human body, being the most cholesterol-rich organ, although consisting in only 2% of the total body mass [5]. Compared to other tissues in the body, the brain presents a 10-fold higher cholesterol concentration [6]**.** In the central nervous system (CNS), cholesterol is primarily unesterified (at least 99%) [2], and is found in the plasma membranes of neurons and glial cells [7]. The major amount of unesterified cholesterol (about 70%) is distributed in the myelin sheets of oligodendrocytes (white matter), and the other 30% is found in the astrocytes and neurons within the plasmalemmal and subcellular membranes (gray matter) [8].

In the periphery, cells obtain cholesterol from *de novo* synthesis and from intracellular uptake of diet-derived cholesterol. However, diet or liver-synthetized cholesterol enriched lipoproteins do not affect cholesterol levels in the CNS, since the blood-brain-barrier (BBB) shows impermeability to plasma lipoproteins. Hence, practically all brain cholesterol originates from *in situ* and *de novo* synthesis in astrocytes and neurons, thought at different levels, throughout development [6, 9-10]. Most of the cholesterol found in the adult brain is metabolically inert, and only 0.02% undergoes a daily turnover. Thus the cholesterol found in the CNS results from a balance between *in situ* synthesis and efflux [11].

Dysregulation of cholesterol homeostasis in the brain has been associated to diverse chronic neurodegenerative disorders of idiopathic origin, such as Alzheimer's disease (AD) and Parkinson's disease (PD), and with genetic disorders such as Huntington's disease (HD), Smith-Lemli Opitz syndrome (SLOS) and Niemann-Pick type C (NPC) disease [12].Therefore, the molecular mechanisms that underlie the association between the alterations in cholesterol metabolism and neurodegenerative disorders is being studied in a variety of disease models. In the cases of the genetic disorders such as SLOS and NPC, there is a direct link between mutations in genes involved in the synthesis or intracellular trafficking of cholesterol and

disease phenotype, respectively**.** Nevertheless, the role of cholesterol in the etiology of age-related neurogenerative disorders is still largely unknown [12].

1.2. Regulation of brain cholesterol homeostasis

Cholesterol homeostasis is regulated by a complex interaction between various proteins that sense and respond to alterations of its levels. The proteins involved can be regulated by cholesterol itself or by its intermediates or derivatives [13].

The synthesis of cellular cholesterol occurs mainly in the endoplasmic reticulum (ER)**,** since it is where most of the machinery necessary for the cholesterol homeostasis is located [13]**.** Cholesterol synthesis is initiated by the conversation of acetyl-CoA to 3-hydroxy-3-methylglutaryl-CoA (HMG-CoA), which is converted to mevalonate by an irreversible reaction catalyzed by the rate-limiting enzyme, HMG-CoA reductase (HMGR) (Fig.1). Mevalonate is then converted, through multi-step enzymatic reactions, into 3-isopenenyl pyrophosphate, farnesyl pyrophosphate, squalene, lanosterol until it is finally converted to cholesterol (Fig. 1) [6].

Cholesterol has a long half-life in the brain, which is estimated to be 4-6 months or 5 years, in rodents and humans, respectively [12]**.** Cholesterol cannot be degraded in the CNS and, in the adult, the rate of cholesterol synthesis may overcome the rate of cholesterol accumulation [12]. Therefore, to avoid variations regarding the steady-state levels, there are mechanisms of cholesterol excretion across the BBB. Indeed, a small fraction (0.02-0.4%) of the cholesterol pool in the brain is eliminated every day [5]. However, since cholesterol itself does not cross the BBB, the major elimination pathway involves the conversion of cholesterol into 24 (S)-hydroxycholesterol (24OHC), the most common oxysterol found in the brain (Fig.1) [6]**.** This pathway corresponds to 40-50% of cholesterol turnover in the brain**,** since 24OHC is capable of crossing the BBB, entering the systemic circulation, being further metabolized in the liver, and eliminated from the body in the bile [6, 14]. The conversion of cholesterol into 24OHC is catalyzed by the cholesterol 24-hydroxylase, a microsomal cytochrome P450, encoded by the *CYP46A1* gene. *In vivo* CYP46A1 is expressed in a subgroup of neurons but is not present in astrocytes [12], and in the adult human brain, cholesterol 24-hydroxylase presents relatively higher expression levels in pyramidal cells located in the cortex and hippocampus, granule cells of the dentate gyrus, and neurons of the thalamus [11]. In studies using wild-type and *Cyp46a1* knockout mice, it has been demonstrated that at least 40% of the cholesterol in the brain is eliminated in the form of 24OHC [14].

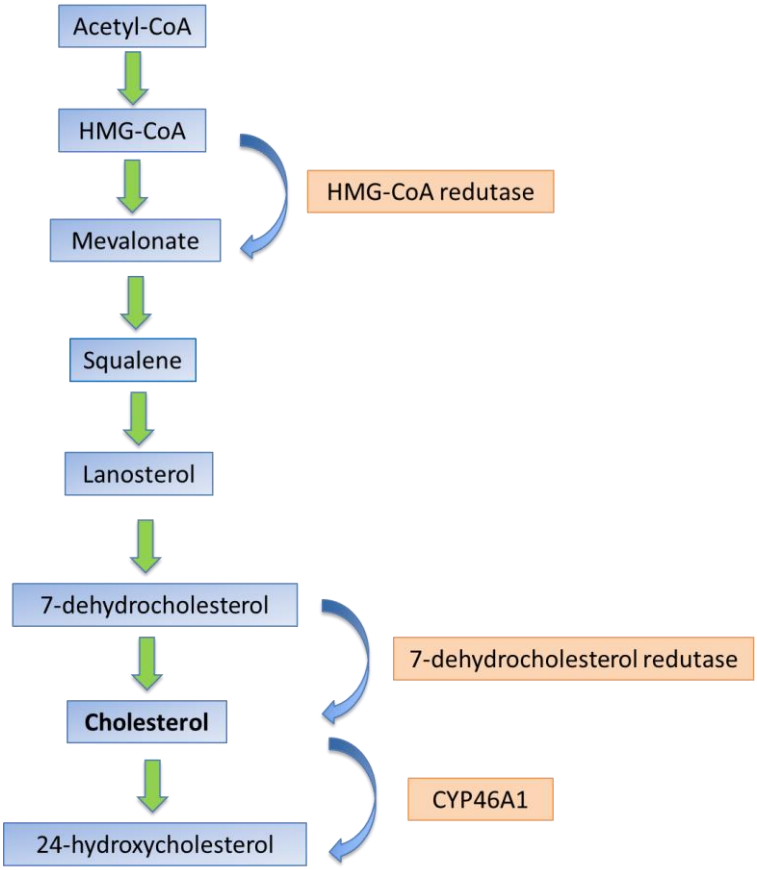

Figure 1- Schematic representation of brain cholesterol synthesis. *The synthesis of cholesterol takes place predominantly in the endoplasmic reticulum (ER), being the conversation of acetyl-CoA to 3-hydroxy-3-methylglutaryl-CoA (HMG-CoA) the first step. HMG-CoA reductase (HMGR), is then responsible for the conversion of the latter to mevalonate which, in its turn, is converted in various species, 3-isopenenyl, pyrophosphate, farnesyl pyrophosphate, squalene, lanosterol until it's finally converted to cholesterol. Cholesterol is then converted into 24 (S)-hydroxycholesterol (24OHC), the most common oxysterol found in the brain, by the cholesterol 24-hydroxylase (CYP46A1), being this the principal elimination pathway of cholesterol in the brain (Adapted from Vance et al., 2012).*

Oxysterols, such as 24OHC are important signaling molecules. They are involved in cholesterol biosynthesis, as they bind to the insulin induced gene (INSIG) protein, and thereby induce the retaining of SREBP cleavage-activating protein (SCAP) in the ER. As a consequence, the major transcription factor involved in the regulation of cholesterolgenic genes, the sterol regulatory-element binding protein 2, (SREBP-2) is retained in the ER, which leads to a downregulation of cholesterol synthesis [6]. Moreover, oxysterols that have a side-chain of hydroxy-, oxo- epoxy- or carboxylate group can act as ligands to Liver X Receptors (LXR). So far, two isoforms of this nuclear receptor have been identified, LXRα and LXRβ, being both proteins expressed in the CNS [15]. These transcription factors directly silence the expression of two key cholesterologenic enzymes (lanosterol 14α-demethylase (CYP51A1), and squalene synthase (farnesyl diphosphate farnesyl transferase 1)), via negative LXR-responsive elements located in the promoter of each of these genes [16]. Moreover, LXRs are activated during cellular cholesterol loading, inducing cholesterol efflux and inflammatory gene repression [17]. Indeed,

they control the expression of ABC transporters and apolipoproteins, as well as the uptake of cholesterol by members of low-density lipoprotein receptor (LDLR) family. Activation of LXR promotes LDLR ubiquitination by the inducible degrader of LDLR (IDOL), therefore further decreasing cellular cholesterol influx [18] .

In the CNS, LXRs play a neuroprotective role, not only by decreasing cholesterol levels, but also by acting on neuroinflammation, since their activation by synthetic agonists results in reduced tissue loss and neuronal death, decreased BBB disruption and brain edema, and decreased microglial activation [19, 20] and pro-inflammatory responses [21]. Indeed, LXR activation decreases the production of numerous pro-inflammatory factors produced by cultured glial cells, such as inducible nitric oxide synthase (iNOS) and nitric oxide, as well as it decreases the nuclear factor kappa B (NF-κB) pathway activity [22–24].

NF-κB is an important regulator of inflammation [25], that mediates several physiological and pathological processes involved in neurodegeneration in the CNS [26]. This transcription factor acts as a dimer, of which p65/p50 heterodimer is the most common, and binds to regulatory common sequence motif, the κB DNA response element in the promoter of its target genes [26, 27]. The classical NF-κB signaling is an important regulator of inflammation since it controls gene expression of several pro-inflammatory cytokines, chemokines, enzymes and adhesion molecules [25]. NF-κB signaling cascade starts when a pro-inflammatory stimulus triggers the phosphorylation and activation of inhibitor of nuclear factor kappa-B kinase subunit beta (IKKβ), which is a subunit of the inhibitor of IκB kinase. Once IKKβ is activated, it phosphorylates inhibitor of nuclear factor kappa B alpha (IκB-α), the IκB inhibitory protein, targeting it for ubiquitination and proteasomal degradation. In the cytosol, NF-κB subunits are then released, form dimers and migrate into the nucleus, where they recognize and bind to their DNA cognate sequences motif in order to promote gene expression [25]. In the promoter of pro- inflammatory genes, binding of NF-κB, in response to the inflammatory stimulus leads to exchange of corepressors and recruitment of coactivators to activate inflammatory gene transcription [28]. LXR activation promotes the specific conjugation of small ubiquitin-like modifier- 2/3 (SUMO-2/3) to its ligand binding domain, and SUMOylated LXRs dock to corepressor complexes at the promoters of inflammatory genes [29], leading to transrepression of gene transcription. In the brain, NF-κB is expressed in neurons and glia and has a very important role in controlling inflammation, but also other aspects of neuronal activity. In glial cells, NF-κB may be activated by cytokines, including Tumor necrosis factor α (TNF-α) and interleukin-1β (IL-1β) through the canonical pathway, leading to, activated microglia, and to the expression and release of pro-inflammatory molecules [30]. Moreover, in neuronal cells, while low concentrations of 24OHC activate LXR transcriptional activity triggering a neuroprotective response [15], high doses have been described to induce necroptosis [31].

Interestingly, it has recently been demonstrated that LXR activation by 24(S), 25-epoxycholesterol can induce neurogenesis of dopaminergic neurons [32]. Moreover, and in

agreement, overexpression of CYP46A1, *in vitro* and *in vivo*, leads to an increase of the levels of 24OHC and 24(S), 25-epoxycholesterol in the developing midbrain, promoting dopaminergic neurons neurogenesis [33]. Oxysterols have also been demonstrated to act as ligands of G protein-coupled receptors (GPCRs) and of N-methyl-D-aspartate receptors (NMDARs) [34].

As previously mentioned, the circulating levels of 24OHC are mostly derived from the brain and depend on the balance between its production and elimination, and also on the metabolization capacity of the liver. Since the levels of this metabolite in the circulation are relatively stable in healthy adults and independent of diurnal variations, under most conditions, this oxysterol has been studied as putative biomarker for brain cholesterol homeostasis as it is probable that it reflects the number of metabolically active neurons [35].

Indeed, it was shown that the plasmatic levels of 24OHC correlate with the progression of neurodegenerative disorders. Patients with advanced AD and vascular dementia show decreased levels of plasma 24OHC, which likely underlines the severe neuronal loss associated with this stage of the disease, and consequently the loss of CYP46A1 expression [36–39]. Not only it might be a possible biomarker for CNS neuronal mass in cases of aggravated neuronal loss, but also reflect demyelinating stages in specific diseases. For example, there is a tendency for higher levels of plasma 24OHC at early stages of Multiple Sclerosis (MS), and a decrease in patients at later stages of the disease [40]. This is in line with the idea that acute episodes of demyelination in MS increase the production and efflux of 24OHC from the brain into the circulation. These episodes are most likely to occur at early stages of the disease. The progressive decay of 24OHC levels with the duration of MS may be related to the loss of CYP46A1 expression due to severe neuronal loss, similarly to what has been hypothesized for AD [40]. However, the correlation might not be so evident since it was not observed changes of 24OHC for other disorders, such as amyotrophic lateral sclerosis or NPC disease [41, 42].

1.3. CYP46A1 and its implication in neurodegenerative disorders

As mentioned previously, CYP46A1 is involved in the main brain cholesterol elimination pathway, which results in the conversion of cholesterol to 24OHC, being an essential enzyme in the cholesterol homeostasis, responsible for half of cholesterol turnover in the CNS [14].

Alterations in CYP46A1 expression levels at an early developmental stage are balanced by homeostatic adaptation of cholesterol metabolism, specially the cholesterol biosynthesis pathway, since it was seen that when CYP46A1 is overexpressed or absent in transgenic lines, the cholesterol levels remain unaltered [11].

In a non-pathological context, there seems to be a correlation between CYP46A1 and high-order brain functions in mice, including memory and learning since increased expression of this hydroxylase improves cognition, while a reduction leads to the opposite effect [43].

We have shown that increasing the CYP46A1 expression stimulates neuronal dendritic outgrowth and protrusion density, increases the expression of synaptic genes and the presence of synaptic proteins in the synaptosomal fraction, both *in vivo* and *in vitro*. These alterations were in accordance with the improvement in cognitive function and the cognitive deficit observed *in vivo* in CYP46A1 transgenic mice and Cyp46a1$^{-/-}$ mice, respectively [44]. Moreover, it has been described that glutamatergic synaptic input leads to loss of cholesterol as a result of higher activity of CYP46A1 [44]. This agrees with our findings demonstrating that cholesterol loss mediated by increased CYP46A1 activity results in higher levels of synaptic proteins and increases dendritic protrusion density [44].

Since it has been demonstrated that modulation of CYP46A1 restores cholesterol homeostasis this cholesterol hydroxylase has been considered an appealing drug target for the treatment of neurodegenerative disorders [43]. Understanding the pathways regulated by this enzyme can lead to the discovery of therapies for neurological disorders where an impairment of cholesterol metabolism has been identified. In that sense, the role of CYP46A1 was initially addressed in AD, where a clear connection between the amyloid production and deregulation of cholesterol metabolism has been demonstrated, since higher levels of membrane cholesterol stimulate the production and deposition of amyloid- ß (Aß) peptides [45, 46].

In order to further investigate whether increased cholesterol levels in neurons is involved in neurodegeneration, Djelti *et al* used an adeno-associated virus (AAV) encoding a short hairpin RNA directed against the mouse CYP46A1 mRNA to inhibit the expression of this gene. As a result, higher cholesterol levels were observed in neurons, as well as cognitive deficits and hippocampal atrophy caused by apoptotic neuronal death [11]. Thus, decreasing CYP46A1 gene expression causes an increase in the levels of cholesterol in neurons, and the resulting cholesterol accumulation causes apoptotic death of neurons and consequent cognitive deficits. It was also observed an increased production of Aß peptides and the abnormal phosphorylation of tau protein resultant from downregulation of CYP46A1 expression, thus proving that cholesterol accumulation sensitizes neurons to AD-like pathology [11]. The decrease in 24OHC levels after AAV-shCYP46A1 injection, led to significant increase of cholesterol at biochemical and cellular levels in the hippocampus. Since the expression levels of the HMGR and SREBP2 remained unaltered, the accumulation of cholesterol resulted from the reduction of the cholesterol efflux and not from an increase of its biosynthesis. In conclusion, it has been shown that silencing of CYP46A1 in the hippocampus of wild-type (WT) mice leads to cholesterol accumulation. The accumulation of cholesterol damages neurons since an increment of cholesterol leads to early AD phenotype and also causes increased neuronal susceptibility to Aß- induced toxicity. Increased amyloidogenesis was accompanied with neuronal death, hippocampus atrophy and cognitive impairment [11].

On the other hand, increased CYP46A1 expression in *in vivo* models of AD and HD, were shown to have a beneficial effect, suggesting that brain gene delivery of CYP46A1 can be of significant therapeutic interest in neurodegenerative disorders. Using a virus-mediated gene

delivery approach *in vivo*, the group of Nathalie Cartier has contributed to elucidate the role of CYP46A1 in the pathophysiology of AD and HD. In a study developed with the objective of investigating the consequences of CYP46A1 ectopic expression on the phenotype of THY-Tau22 mouse, which is a model of AD-like Tau pathology where amyloid pathology is absent. Once again, an AAV gene transfer was used as a strategy to increase CYP46A1 expression. It was observed that injection of the AAV-CYP46A1 vector into the hippocampus of THY-Tau22 mice resulted in the normalization of CYP46A1 levels and 24OHC content. Importantly, in mice overexpressing CYP46A1 the cognitive deficits, impaired long-term depression and spine defects that characterize the THY-Tau22 model were completely rescued, whereas Tau hyperphosphorylation and associated gliosis were unaffected [45].

In another study, AAV encoding CYP46A1 was injected in the cortex and hippocampus of APP23 mice, a different genetic model for AD. In this mice model there was a relevant reduction of Aß pathology caused by neuronal expression of CYP46A1, before or after the onset of amyloid plaques. Improvement of cognitive performance was also observed, since at 6 months of age APP23 mice showed improvement of spatial memory, before the onset of amyloid deposits. A two-fold increase of 24OHC levels in the brain and reduction of microgliosis and astrogliosis was detected when animals were injected with the CYP46A1 AAV5 encoding vector [46]. Nevertheless, it is unclear if the observed decrease in microgliosis and astrogliosis is due to a decrease in cholesterol loading, or due to the activation of LXR, since a specific up-regulation of LXR- target genes was not observed. This hypothesis cannot however be completely excluded, since in different mice models of AD, LXR activation has led to a decreased synthesis of pro-inflammatory factors that may result from the deactivation of the NF-κB pathway [47].

Other studies from Cartier's Lab have focused on the targeting of CYP46A1 in other neurodegenerative diseases. For instance, in a study focused on HD, in which accumulation of cholesterol has been implicated in striatal neurons, CYP46A1 expression was knocked down in the striatum of WT animals. This resulted in a HD phenotype, including spontaneous striatal neuron degeneration and motor deficits. On the contrary, restoring CYP46A1 by AAV infection, in the R6/2 HD mouse model, resulted in amelioration of motor deficits, improved medium spiny neuron and restored cholesterol homeostasis [48]. Recently, it was also shown that in a transgenic Spinocerebellar Ataxia 3 (SCA3) model, with a severe motor phenotype, cerebellar delivery of AAVrh10-CYP46A1 is strongly neuroprotective in adult mice with established pathology. CYP46A1 significantly decreases ataxin-3 protein aggregation, alleviates motor impairments and improves SCA3-associated neuropathology [49].

In 2008, Irina Pikuleva's Lab published the substrate-bound and substrate-free CYP46A1 crystal structures [50], which allowed the identification of compounds that act as CYP46A1 substrates, activators or inhibitors. Phenacetin, 4'-(2-hydroxyethoxy)-acetanilide and acetaminophen were reported as *in vitro* activators [50], while clobenpropit, thioperamide, tranylcypromine and fluvoxamine were identified as *in vitro* inhibitors [50, 51]. It has also been demonstrated that the

antifungal drug voriconazole can inhibit CYP46A1 activity *in vivo* and *in vitro* [52]. Importantly, the anti-human immunodeficiency virus drug efavirenz has been shown to increase CYP46A1 activity *in vitro* and *in vivo*, leading to an increase in brain cholesterol turnover, without changing cholesterol levels. These results led Pikuleva and coworkers to test a very low daily dose of efavirenz on 5XFAD AD mice [53]. Efavirenz treatment started from three months of age, after amyloid plaque appearance, and continued for 6 months. This treatment led to CYP46A1 activation in the brain, enhancement of brain cholesterol turnover, behavioral improvements, reduction in microglia activation but increased astrocyte reactivity [53].

During the development of our work, Mitroi and collaborators showed that efavirenz oral treatment ameliorates brain pathology in NPC1^{nmf164} mice. Indeed, this study suggested that pharmacological activation of CYP46A1 normalizes synaptic levels of cholesterol, long term potentiation and cognitive abilities, and extends lifespan of these NPC mice [54].

Although the therapeutic potential of CYP46A1 activation has been extensively investigated, the effects of CYP46A1 inhibition remain poorly characterized. Martín-Segura *et al.* (2019) described that age-associated cholesterol reduction triggers brain insulin resistance by facilitating ligand-independent receptor activation and pathway desensitization [55]. Interestingly, *in vivo* inhibition of CYP46A1 using voriconazole, led to improvement of insulin signaling in old mice [55]. Moreover, in a very recent study, soticlestat was used to inhibit CYP46A1 in the APP/PS1-Transgenic (Tg) mouse model of AD. These mice, with excitatory/inhibitory imbalance and short lifespan, yielded a remarkable survival benefit when bred with *Cyp46A1*-knockout animals. Soticlestat lowered brain 24OHC levels in a dose-dependent manner and substantially reduced premature deaths of APP/PS1-Tg mice at a dose lowering brain 24OHC by approximately 50%. Furthermore, microdialysis experiments showed that soticlestat suppressed potassium-evoked extracellular glutamate elevations in the hippocampus. Taken together, this study suggests that using soticlestat to reduce 24OHC levels can be used as a therapeutic approach when there is excitatory/inhibitory imbalance in the brain [56].

Further investigation is needed in order to understand the mechanisms involved in the beneficial effects that result from increasing the expression or activity of CYP46A1. Indeed, CYP46A1 is involved in cholesterol levels and turnover, as well as in the production of 24OHC, being able therefore to modulate various pathways in neurons [43]. Considering that accumulation of cholesterol is linked to neuronal pathologies, it seems that one of the possible mechanisms is directly decreasing the levels of cholesterol in specific membrane domains. It is also possible that the increased production of 24OHC can be involved in the beneficial effects since there are *in vitro* studies that demonstrate that 24OHC can reduce the content of Aß [57, 58]. Another mechanism that should be considered is the increase in cholesterol turnover, which is reflected by an increase in the levels of several intermediates of the mevalonate pathway, that are essential for the activity of small guanosine triphosphate-binding proteins (sGTPases), essential in neuronal development [43].

1.4. Niemann-Pick type C (NPC) disease

1.4.1. NPC disease

NPC disease is a fatal neurodegenerative disorder. It is an autosomal recessive lysosomal storage disorder relatively rare, with an estimated incidence of 1:150,000 in western Europe [59, 60]. NPC patients are usually children with progressive impairment of motor and intellectual function presenting various symptoms such as cerebellar ataxia, dementia, dysphagia, dysarthria and hepatosplenomegaly [61]. The clinical onset for NPC can be broad, including the periods from infancy to adulthood, although there can be acute cases in the perinatal period or even in utero, in rare cases [62]. This disorder causes premature death, since the patients usually die within the first two decades of life [63] .

In NPC disease, the more severe defects are observed in the CNS rather than in the peripheral tissues [61], and the most noticeable histological feature observed in *post-mortem* brains of NPC patients is the severe death of neurons, in particular Purkinje cells in the cerebellum. This is consistent with the impairment of motor function observed in these individuals [63]. Since Purkinje cells are the only neurons projecting out of the cerebellar cortex, their extensive loss is directly related to severe ataxia. Purkinje cell death is preceded by cholesterol storage, meganeurite formation, axonal swellings and stunted dendritic arbors, consisting of representative signs of a progressive process of neurodegeneration [64]. It is still not understood the reason why the brain is the most affected organ in NPC disease, since the Niemann–Pick C1 protein (NPC1) and Niemann-Pick type C2 protein (NPC2) protein are generally expressed in animal tissues [12].

NPC results from loss of function mutations in the NPC1 or NPC2 genes, in 95% and 5% of the cases, respectively [60]. NPC1 encodes the large 13 transmembrane domain NPC1 protein, composed by 1278 amino acids, which is located in the limiting membrane of late endosomes and lysosomes and plays a fundamental role in intracellular cholesterol trafficking [60, 62]. NPC2 encodes a small luminal protein that binds cholesterol and transfers it to NPC1 [60, 65].

In NPC disease, a correlation between alterations in cholesterol metabolism in the brain and neurodegeneration has been observed. NPC1 and NPC2 proteins both bind to cholesterol in late endosomes/ lysosomes in order to facilitate the elimination of unesterified cholesterol resulting from endocytosed lipoproteins [66]. NPC2 binds and carries cholesterol in the luminal space of the late endosome/ lysosome and transports it to the N-terminal domain of NPC1 (Fig. 2) [59, 61]. This protein binds unesterified cholesterol within the lysosome, interacting with NPC2 and facilitating cholesterol exportation from the lysosome. It is still unclear how the NPC1 and NPC2 proteins interact, how they sense the concentration of lipids within the lysosome and why NPC1 follows the vesicular cargo to its destination. It has been suggested that the initial

sphingolipids accumulation causes alteration of the calcium levels in the lysosome, which triggers the cascade of secondary effects that is observed in NPC [59].

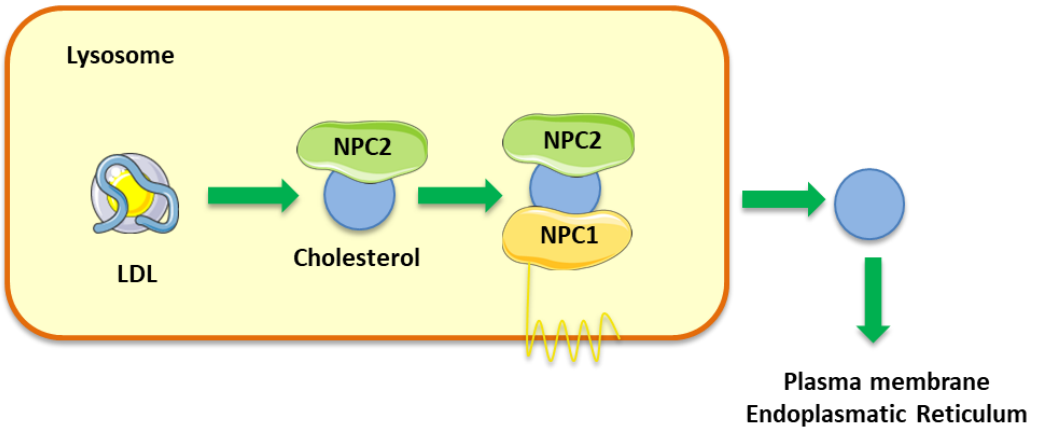

Figure 2- Cholesterol export from late endosomes/lysosomes mediated by NPC1 and NPC2. *Endocytosed LDLs release unesterified cholesterol into the luminal space of the late endosome/ lysosome, where NPC2 binds to cholesterol, transporting it to the membrane. NPC1 then binds to cholesterol and interacts with NPC2 resulting in cholesterol exportation. Cholesterol is then transported to the ER and plasma membrane (Adapted from Vance et al., 2012)*

As a result of mutations in NPC1 or NPC2, in NPC1 or NPC2-deficient cells, occurs an impairment of low density lipoprotein (LDL) cholesterol esterification and reduction in trafficking of unesterified cholesterol to the plasma membrane [60]. Thus, unesterified cholesterol and other lipids, including glycosphingolipids, which are more protuberant in neuronal tissue, and sphingomyelin and sphingosine, are sequestered in late endosomes/ lysosomes [60, 62]. This causes a reduction of the amount of cholesterol in the plasma membrane and ER. Considering the importance of cholesterol in the maintenance of the plasma membrane order, the reduction of membrane cholesterol can lead to membrane dysfunction or even trigger apoptosis [59]**.** Deficiency in NPC1 or NPC2 results in inhibition of the transport of LDL-cholesterol from the lysosome to the ER, leading to activation of the expression of genes involved in the synthesis of cholesterol and an increased expression of lysosomal genes derived from lysosomal dysfunctions [61]. The filipin test is the standard NPC diagnostic method performed on cultured fibroblasts. Filipin staining allows detecting, in cells, the sequestration and consequent accumulation of unesterified cholesterol in the late endosomes/lysosomes by fluorescence microscopy. Filipin enables the detection of unesterified cholesterol in biological membranes since it consists of a polyene antibiotic that binds to cholesterol but not to esterified sterols [67].

The cholesterol accumulation has been associated with oxidative stress, which has been reported as a potential pathological mechanism in NPC disease, since *in vitro* and *in vivo* mouse studies suggest the presence of increased oxidative stress in NPC. This was also found in serum from NPC patients [68]. Moreover, defects in autophagy have also been implicated in NPC disease as well as in other neurodegenerative and liver disorders. However, the nature of autophagy dysfunction in human cells affected by NPC disease has not yet been fully

determined [69]. Nevertheless, it has been shown that defective autophagy in NPC1 disease is associated with cholesterol accumulation, where the maturation of autophagosomes is impaired because of defective amphisome formation caused by failure in soluble N-ethylmaleimide-sensitive factor attachment protein receptors (SNARE) machinery, whereas the lysosomal proteolytic function remains unaffected. Expression of functional NPC1 protein can rescue this defect [70].

Neuroinflammation is also a key feature in NPC and is found in most neurodegenerative disorders. In the CNS, the first line of defense consists of the innate immune system of microglia, astrocytes and perivascular macrophages [71]. Microglia consists of resident immune cells that monitor the neuronal environment and are activated in case of pathogenic triggers. Upon activation, microglia moves in the direction of the pathogenic focus detected, proliferate and secrete pro-inflammatory cytokines, and phagocytose cellular debris. Microglia can also release growth factors and anti-inflammatory cytokines, playing a reparative and neuroprotective role [72]. Activation of microglia and astrocytes leads to a morphological change that can be characterized by specific markers, such as positive staining for Ionized calcium-binding adapter molecule 1 (Iba-1) and Cluster of Differentiation 68 (CD68), and Glial Fibrillary Acidic Protein (GFAP), respectively [71] .

In NPC1 disease chronic inflammation and activation of glial cells has also been reported. Accumulation of peripheral immune cells into the CNS often occurs simultaneously due to BBB leakage. As a consequence of secretion of pro-inflammatory cytokines, including IL-6, IL-1β and TNF-α by activated microglia [73], which is a nonspecific response to the damage of the surrounding cells, such as neurons and other glial cells, these cells then release damage associated molecule patterns (DAMPs), which can lead to adverse glial cell activation, which, in turn, creates a self-propagating cycle of neuroinflammation, promoting cell death [74, 76].

Unesterified cholesterol accumulation may not be sufficient to induce microglial activation, since at birth when there is already significant accumulation of unesterified cholesterol there is a very low level of microgliosis. This suggests that other activating signals such as neuronal cell death, are crucial to trigger neuroinflammation [73]. Indeed, in the $Npc1^{nih}$ mouse model, activation of microglia starts at approximately 2 weeks after birth, as the first sign of neuroinflammation concomitant with the neurodegenerative cascade. Marked activation of astrocytes occurs later, at approximately 4 weeks after birth, underneath the Purkinje cell layer corresponding to the regions of early apoptosis observed in the disease [71]. In the $Npc1^{nih}$ knockout mouse model, it was observed that microglia and astrocytes activation occurs mainly in the thalamus and cerebellum, the brain regions where neuronal death mainly occurs, in later stages of the disease [72]. This suggests that astro- and microgliosis occur in the vicinity of dying neurons in NPC. However, it is still not fully understood how inflammation impacts NPC disease progression since it is yet to be determined if neuroinflammation is a primary pathological process of the disorder or a secondary process caused by initial genetic and trafficking defects

that culminate in neuronal cell death. However, recent studies suggest that neuroinflammation is a secondary process observed in NPC1 disease [71].

Currently there is no effective treatment approved by the Food and Drug Administration (FDA) for treating NPC disease. Nevertheless, due to use of animal models of NPC disease it has been possible to develop treatment options that are able to slow the progression of NPC [62].

In Europe and other countries, orally administered substrate reduction therapy using N-butyldeoxynojirimycin (miglustat, ZavescaVR) is approved in NPC individuals for the treatment of progressive neurological manifestations. Miglustat causes reduction of glycosphingolipids levels since it functions as a partial inhibitor of the glucosylceramide synthase. Stabilization in diverse neurological parameters and in some cases even improvement due to long term use with miglustat have been described in a study of the International Registry for NPC. Due to improved swallowing and reduced frequency of aspiration pneumonia, it was observed a longer lifespan since these correspond to a frequent cause of death in NPC individuals. Despite the beneficial effects observed in NPC patients, miglustat presents side effects, such as osmotic diarrhea. Thus, it is not approved as a therapeutic method for NPC disease in the USA [62].

A novel therapeutic approach for NPC disease has emerged from studies in pre-clinical models, consisting of a single subcutaneous injection of cyclodextrin, a cholesterol-binding compound. Cyclodextrin administration in 7-day-old $Npc1^{-/-}$ mice has been shown to reduce neurodegeneration and increase lifespan of the mice by about 50% [77]. Since cyclodextrin is a compound that presents low toxicity and has been used as a drug delivery vehicle in humans, it was administered as a treatment in limited cases of NPC disease [12]. 2-hydroxypropyl-beta-cyclodextrin (HP-β-CD) is an oligosaccharide frequently used as a drug excipient to deliver insoluble drugs. It was verified that intra-ventricular administration of this oligosaccharide to the CNS in NPC mice not only slowed the progression of the disease but also led to the decrement of Purkinje cell death and a reduced rate of accumulation of cholesterol and sphingolipids. Since HP-β-CD is unable of crossing the BBB successfully, an invasive intrathecal administration via lumbar puncture every 2 weeks in a clinical trial is necessary. So far, ototoxicity has been described as a side effect [62].

It has also been demonstrated that treatment with histone deacetylase (HDAC) inhibitors is able to increase expression of the $NPC1^{I1061T}$ mutant protein, which presents lower activity than the NPC1 WT protein. The expression of the mutant protein is increased enough to correct the defect in cholesterol efflux from endosomes and lysosomes [78]. We have also demonstrated that HDAC inhibitors up-regulate *CYP46A1* gene transcription [79], and in a pharmacologic cellular model of NPC, we have shown that treatment with Trichostatin A can ameliorate the disease phenotype by restoring the expression of key genes involved in cholesterol synthesis, uptake and efflux and promoting lysosomal cholesterol redistribution [79]. So far, LBH589 (panobinostat), an HDAC inhibitor capable of crossing the BBB, has been described as the most effective in correcting the NPC disease phenotype [78].

AAV vectors are the leading platform for gene delivery for the treatment of a variety of human diseases. This type of vector presents reduced immunogenicity and risk of insertional mutagenesis and can also mediate long-term gene expression in dividing and non-dividing cells, making them promising gene delivery vehicles. AAV vectors have been used in various CNS clinical studies since neurons are post-mitotic and long-term transgene expression is needed in various chronic neurological diseases. AAV can target specific cell types and regions in the CNS that are involved in neurological disorders, which is crucial for safe and effective therapeutic strategies [80].

There are several therapeutic routes of administration of AAV used in CNS disorders: intracranial, which is the most used; intracisterna magna and intracerebroventricular injections into the cerebrospinal fluid. There are also intracarotid and intravenous injections into the bloodstream and intrathecal administration, which is a dorsal injection into the cerebrospinal fluid [80].

Gene therapy using AAV administered to the CNS as potential treatments for neurodegenerative lysosomal storage disorders has been translated from pre-clinical studies to clinical trials. It has been shown that AAV, particularly serotypes 9 and rh10 are able to cross the BBB and to transduce cells in the CNS, particularly neurons [60]. Indeed, two pre-clinical studies using AAV9 delivery of NPC1 have been published, and in both studies, the vector was administered via systemic intravenous or intracardial injection, and the capability of AAV9 to cross the BBB was proven [62]**.** The NPC1 protein has a transmembrane domain and mechanisms of cross-correction of neighboring cells by membrane proteins have not been reported. Therefore, in NPC, the route of administration of the vector is extremely important, since the efficacy of gene therapy for this disease depends on the optimal direct transduction of a quantity of cells as higher as possible in the brain [62]. These first pre-clinical studies to prove that AAV9 gene delivery is an efficient option to treat NPC disease demonstrated that ectopic expression of NPC1 protein caused improved clinical features such as delayed weight loss, considerably extended lifespan, decreased cholesterol storage, and reduced Purkinje cell loss degeneration [60].

1.4.2. Experimental models of NPC

The NPC1 gene is highly conserved in eukaryotic organisms, allowing the generation of various experimental models, such as cat, mouse, zebrafish, fruit fly, nematode and yeast models of NPC [81]. However, as for other diseases, there is a preference for NPC1 mice models, due to its increasing ease of genetic manipulations and the relative cost efficacy [82].

There are several animal models for NPC1 disease, including the BALB/cNctr-Npc1^{m1N}/J, a well-characterized murine model derived from a spontaneous mutation in the Npc1 gene [60].

NPC1 protein is almost totally absent in this model, causing the Npc1$^{-/-}$ (BALB/cNctr-Npc1^{m1N}/J) mouse to exhibit all the hallmarks of the disease, since mice that are homozygous for the Npc1 mutant allele (Npc1$^{-/-}$) are null and unable to produce a functional protein [60, 83]. These mice exhibit the most severe and rapidly progressing disease, showing weight loss, ataxia and consistent lethality within NPC laboratory colonies [60]. Npc1$^{-/-}$ mice display neuropathological manifestations resembling what is observed in NPC1 individuals, including lipid and cholesterol accumulation in the neurons and glial cells and Purkinje cell loss in the cerebellum [60]. Taking this into consideration, Npc1$^{-/-}$ mice corresponds to an adequate model to represent NPC1 disease caused by loss of function mutations in NPC1 [60]. Various neuropathology studies developed in the Npc1$^{-/-}$, BALB/cNctr-Npc1^{m1N}/J, model showed neurodegeneration in various areas of the brain, such as thalamus, substantia nigra, cortex and the cerebellum, being the cerebellar Purkinje cells the most affected. Cell death is accompanied by an inflammatory response mediated by microglia and astrocytic activation and accumulation of cholesterol and sphingolipids [62]. In Npc1$^{-/-}$ neurons, neuronal cell bodies present a higher amount of cholesterol while distal axons have a lower amount [84]. Thus, the deficiency of cholesterol in axons can lead to some of the neurological deficits observed in NPC disease. Synaptic function can also be damaged in Npc1$^{-/-}$ neurons, since the deficiency of cholesterol decreases the exocytosis of synaptic vesicles [85]**.**

Another well-characterized null animal model is the Npc1^{nih} mouse. The Npc1^{nih} model displays many of the clinical, pathological and biochemical hallmarks of NPC and, in particular, reproduces the clinically important symptoms of ambulation challenges and loss of motor coordination, while also presenting demyelination and a biomarker profile reflecting many of the biological changes also observed in human patients [83].

While the previously described mouse models will continue to be of central importance for NPC drug discovery and development, these are essentially null models. Thus, it is useful for testing various therapeutic concepts such as replacement strategies (e.g. gene therapy), metabolite storage reduction (e.g. cyclodextrins and miglustat), lysosomal augmentation, and anti-inflammatory and combination therapies [reviewed in 82]. However, it does not replicate one of the fundamental aspects of NPC biology, the misfolding and loss of function of NPC1 protein as a consequence of missense mutations, which constitute the majority of mutations in NPC.

To this end, other models such as the Npc1^{nmf164} and Npc1^{I1061T} mouse models have been developed that could allow testing various chaperoning and proteostasis targeted strategies including proteasome inhibition and modulation of cellular molecular chaperones.

The Npc1^{nmf164} mouse model was generated using ethyl-nitrosourea mutagenesis [86]. In this model, the NPC1 protein has a point mutation, originating a D1005G mutation. This mutation is located in the large cysteine-rich luminal loop of the NPC1 protein, which is a mutational hotspot where the two most frequent pathological NPC1 mutations encoding the P1007A and I1061T missense mutations are found. Npc1^{nmf164} mice have a less severe phenotype than Npc1 null,

which correlates with the partial loss of functional NPC1 protein [87, 88]. Thus, it is possible to test therapies that can improve the stability of the protein [86].

NPC1 protein levels are mainly regulated by translational or post-translational mechanisms rather than transcriptional mechanisms since there was no connection found between transcript and mutant protein levels in patients fibroblasts [89]. Indeed, the most common human mutation, NPC1I1061T, corresponding to 15–20% of all disease causing alleles, encodes a misfolded protein that, because of ER-associated degradation, has a reduced half-life [90]. As previously mentioned, some therapies have been developed directed at stabilization of the mutant NPC1 protein that result in reduced cholesterol storage in patient fibroblasts. To test these therapies *in vivo*, the group of Daniel S. Ory has developed the $Npc1^{tm(I1061T)Dso}$ knock-in mouse model [91]. These mice exhibit less severe and delayed manifestations of NPC1 disease, including weight loss, motor coordination, Purkinje cell loss, lipid storage, and premature death, when compared to the $Npc1^{-/-}$ model [91]. The NPC1I1061T protein produced by the $Npc1^{tm(I1061T)Dso}$ model has a reduced half-life *in vivo*, due to protein misfolding and rapid ER-associated degradation, however it can be stabilized by histone deacetylase inhibition [91].

Since NPC disease is very complex, there is not a single model capable of covering all the pathological aspects of the disease. Therefore, one should evaluate the available models to choose the most suitable model for the study objective [81].

2. Objectives

NPC disease is a fatal neurodegenerative disorder with limited treatment options. Taking into account the role of CYP46A1 in cholesterol elimination and neuronal function, we hypothesized that it could be a potential therapeutic target in NPC disease.

Indeed, our preliminary results show that cholesterol levels and more importantly, cholesterol accumulation in late endosomes/ lysosomes is robustly reduced upon CYP46A1 ectopic expression in different NPC cellular models, namely in patients' fibroblasts. This effect was also accompanied by partial normalization of the mRNA levels of several genes involved in cholesterol homeostasis and by the rescue of mitochondrial function and integrity which were greatly deregulated in NPC (Costa et al, unpublished results).

Therefore, we aim to determine if CYP46A1 overexpression *in vivo* can decrease neurotoxicity in NPC1 mice brain and improve the disease phenotype, by delivering AAV-CYP46A1 to the cerebellum of $Npc1^{tm(I1061T)}$ mice. Improvement in molecular and neuropathological hallmarks of NPC disease was characterized as well as improvement in motor function.

Specifically, the amelioration of neurological hallmarks of NPC disease was evaluated, by determining Purkinje cell neuronal loss, and the protein expression levels of neuroinflammatory markers in the cortex and cerebellum.

Moreover, to determine the effect of CYP46A1 ectopic expression on disease progression rotarod and catwalk gait analysis, which has been previously validated in NPC1 mouse models, was used to determine the evolution of motor coordination deficits.

3. Materials and Methods

3.1. Animals and Treatment

All animal experiments were performed according to the 2010/63/EU Directive and National law (Decreto-Lei nº 113/2013). Animal facilities and the people involved in animal experiments are certified by the Portuguese regulatory entity, Direcção Geral de Alimentação e Veterinária (DGAV). All the protocols executed were submitted to the Animal Welfare Committee (ORBEA) of IMM animal ethics committee and to DGAV. All animal experiments will be designed and conducted with commitment to the 3Rs.

Homozygous mutants ($Npc1^{tm(I1061T)}$) and wild-type littermates ($Npc1^{+/+}$), were generated by crossing heterozygous mutant males and females, in-house (https://www.jax.org/strain/027704). Mice, 13 females and 11 males, were housed on a 12-h light–dark cycle with free access to standard diet and water *ad libitum*, under standardized conditions. Group consisting of WT littermates ($Npc1^{+/+}$) and $Npc1^{tm(I1061T)}$ homozygous mice were anesthetized by isoflurane inhalation. At 5 weeks of age, a group of $Npc1^{+/+}$ mice (5 males and 4 females) received a retro-orbital injection with a dose of $5x10^{11}$ vg (viral genomes) of AAVPHPeB.HA.GFP (WT-GFP), while to a group of $Npc1^{tm(I1061T)}$ mice (3 males and 4 females) was administered an equal dose of the same vector (NPC-GFP). A third group of $Npc1^{tm(I1061T)}$ mice (3 males and 5 females) received a retro-orbital injection with an equal dose of AAVPHPeB.HA.CYP46A1 (NPC-CYP).

Mice were monitored daily, in order to evaluate their growth. They were weighed weekly from 5 weeks of age, and throughout the duration of the experience. At week 6, and every two weeks, mice balance and motor coordination were assessed with the catwalk and rotarod tests, as described below. Mice were euthanized at week 12 and brain tissues were quickly collected. To minimize the number of animals used, each brain was divided in two. One hemisphere was immediately fixed in 4% paraformaldehyde (PFA) solution, and then further impregnated in gelatin and frozen to be processed for histology. From the other hemisphere we have isolated cortex and cerebellum, and these brain regions were immediately frozen at -80ºC, for future protein and RNA isolation.

3.2. Rotarod test

Mice were tested in a rotarod apparatus specific for mice (Panlab, Harvard Apparatus, Barcelona, Spain) to evaluate their motor performance, from week 6 to week 12. Retention time was measured in animals subjected to 3 trials, in 2 consecutive days, on a constant 10 rpm rotating drum, for a maximum of 180 seconds per attempt. The latency to fall was registered by the investigator and the best performance is presented for each time point.

3.3. Catwalk test

To analyze gait and motor impairment a catwalk test was performed every 2 weeks, from week 6 until week 12. Each animal was placed in a transparent catwalk and its gait in spontaneous locomotion was recorded using a video camera (Webcam Logitech Brio 4K UHD) placed under the catwalk. Mice moved freely for a maximum of 4 minutes. Data obtained from a maximum of three runs was used to determine the average walking speed to cross a stretch of 20 cm in length in the catwalk. Subsequent analysis of the collected recordings was used to determine the stride length for each limb: right and left fore and hindlimbs.

3.4. Protein Extraction

In order to have homogeneous samples of mice brain, frozen tissues isolated from the different brain regions, in this case, cortex and cerebellum were grinded in liquid nitrogen with mortar and pestle. The collected grinded tissues were separated and used for DNA, RNA and protein isolation.

The frozen dissociated tissue was homogenized in lysis buffer (20mM Tris-HCl (pH 7.5), 150mM NaCl, 1mM Na2EDTA, 1mM EGTA, 1% Triton, 2.5mM sodium pyrophosphate, 1mM β-glycerophosphate, 1mM Na3VO4, 1µg/ml leupeptin, supplemented with Complete Mini Protease Inhibitor Cocktail, 200mM Na3VO4 and 1M NaF), incubated on ice for 1 h and centrifuged at 3,000*g* for 10 min, at 4ºC. After 4 times sonication for 4 sec each, samples were centrifuged at 13,000*g* for 15 min, at 4ºC, and the supernatants were collected, flash-frozen and stored at -80°C.

To increase the number of samples and targets analyzed, we have also prepared protein extracts from organic phases obtained after RNA isolation with TRIzol [92]. Briefly, 200µL/mL TRIzol of ethanol 100% were added to each sample tube containing the organic phases. The tubes were homogenized by inversion, incubated at room temperature for 2-3 min and centrifuged at 2,000*g* for 5 min, at 4°C. The supernatants were collected and 150µL/mL TRIzol of isopropanol was added to the tubes, and proteins were precipitated after homogenization and incubation at room temperature for 10 min. The samples were then centrifuged at 12,000 *g* for 10 min, at 4 °C, and the supernatant was discarded. The protein pellets were washed for 3 times with 2mL/mL TRIzol of 0.3M guanidine in 95% ethanol. Subsequently, the samples were incubated at room temperature, for 20 min with vigorous agitation, followed by centrifugation at 7,500*g* for 5 min, at 4°C, and the supernatants were discarded. After the washing steps, 2mL of ethanol 100% was added to each tube and the protein pellets were vortexed. Subsequently, the samples were incubated at room temperature for 20 min and centrifuged at 7,500*g* for 5 min, at

4°C. The supernatant was removed and the pellets were air dried and resuspended in 150μL (the volumes were adjusted to the size of the pellet obtained) of 1:1 solution of 8M urea in Tris-HCl pH 8.0 and 1% sodium dodecyl sulphate (SDS). The samples were submitted to 5 cycles of 15 sec sonication, with an amplitude of 80% and a pulse of 90%, and 30 sec of ice incubation, followed by a centrifugation at 10,000*g* for 5 min, at 4°C. The supernatants containing the protein extracts were collected and kept at -80ºC until further use.

Protein concentration of all the samples was determined using the Bradford method, according to the manufacturer's protocol.

3.5. Western Blotting and Immunodetection

Protein samples were added (5:1) to denaturing buffer (0.25mM Tris-HCL, pH 6.8, 4% SDS, 40% glycerol, 0.2% bromophenol blue, 1% β-mercaptoethanol) and boiled for 5 min. The same amount of protein (50μg) were resolved on 12.5% or 10% sodium dodecyl sulphate-polyacrilamide gel electrophoresis, and the gels were run in 25mM Tris base, 192mM glycine and 0.1% SDS with a fixed amperage of 35mA per gel and electrotransfered to polyvinylidene fluoride membrane with a fixed amperage of 500mA. The membranes were then stained with Amido black 1X for 4 min, washed with destaining solution (25% isopropanol and 10% acetic acid) for 5 min, and dried at room temperature. After re-hydration with ethanol for 1 min, wash with water for 2 min and equilibrate for 5 min in tris-buffered saline-tween (TBS-T) (20mM Tris-Cl pH 7.6, 150mM NaCl, 0.1% Tween-20), the membranes were blocked for 1 h with 5% low-fat milk in TBS-T and then incubated with the specific primary antibodies, namely anti-NPC1, -CYP46A1, -GFAP, -Microtubule-associated protein 1A/1B-light chain 3B (LC-3), -Iba-1 , -IκB-α, -NF-κB and -Glyceraldehyde 3-phosphate dehydrogenase (GAPDH), overnight at 4°C, with shacking, in the conditions indicated in Table 1. After being washed 3 times with TBS-T, for 15 min each, membranes were incubated with anti-mouse or anti-rabbit secondary antibodies conjugated with horseradish peroxidase (HRP) (1:5000) for 1 h at room temperature. The membranes were then washed 3 more times in TBS-T for 15 min each and the immunocomplexes were visualized by chemiluminescent detection with ECL Western blotting detection reagent or SuperSignal® West Femto Maximum Sensivity Substrate in a ChemiDoc™ MP imaging system from Bio-Rad Laboratories (Hercules, CA, USA). GAPDH and amido black staining was used as loading control. The relative intensities of protein bands were analysed using the Image Lab™ analysis software from Bio-Rad Laboratories (Hercules, CA, USA).

Table 1-Antibodies used in Western Blot analysis. *Antibodies were used with the dilution indicated in Western Blot analysis as described in materials and methods.*

Antibody	Comercial Source	Reference	Host	Diluition (WB)
CYP46A1	Santa Cruz Biotech	sc-136148	Mouse (mAb)	1/500
GAPDH	Santa Cruz Biotech	sc-32233	Mouse (mAb)	1/5000
GFAP	Milliore	MAB360	Rabbit	1/1000
IκB-α	Santa Cruz Biotech	sc-1643	Mouse	1/500
Iba-1	Wako Pure Chemicals	019-19741	Rabbit	1/200
LC3	Thermo Fisher Scientific	PA1-16931	Mouse	1/2000
NF-κB (p65)	Santa Cruz Biotech	sc-372	Rabbit	1/500
NPC1	Novus Bio	NB400-148	Rabbit	1/1000

3.6. Cresyl violet staining

Cryostat sagittal 12µm thick mice brain slices with were stained with Cresyl Violet, a standard histological stain for neurons. Briefly, sections were air-dried and stained with filtered Cresyl Violet at 60°C, for 3 min. Subsequently, sections were differentiated in 96% ethanol with 10% acetic acid for 30 sec, and then dehydrated in 100% ethanol and xylene, for about 30 sec in each solution. Finally, sections were mounted with Entellan mounting medium and air-dried.

3.7. Histological analysis and Purkinje cell counts

The brain hemisphere for immunohistochemistry was immediately fixed in PFA 4% for 24 to 48 hours. Afterwards, the hemispheres were sequentially transferred to a 15% and 30% saccharose solution for 24 hours each. The tissue was then embedded in gelatin and frozen at -80ºC for further processing in the cryostat.

The number of Purkinje cells in each brain section was obtained for each of the individual cerebellar lobes (I-X), using 12µm thick midline sagittal brain sections stained with Cresyl Violet. Purkinje cells were manually counted using an EVOS FL Auto 2 microscope under a 40X objective. The length of the Purkinje cell layers was manually traced and measured using ImageJ software analysis (National Institutes of Health). The results are presented as number of Purkinje cells/ mm, reflecting the number of cells per length of cell layer for each cerebellar lobe.

The thickness of granular and molecular cerebellar layers was determined manually measuring the thickness of each layer in each lobe using the ImageJ software analysis.

3.8. Statistical analysis

GraphPad Prism 9. was used to perform statistical analysis. To test if data fit in a normal distribution, Shapiro-Wilk test was performed. One-way ANOVA, followed by Tukey's multiple comparisons test, was used when data fit in a normal distribution. When data failed to pass the normality test, a Krustal-Wallis test was performed, followed by Dunn's multiple comparisons test.

4. Results

4.1. CYP46A1 ectopic expression in Npc1$^{tm(I1061T)}$ mice

Taking into account the role of CYP46A1 in cholesterol elimination and neuronal function, we hypothesized that it could be a potential therapeutic target in NPC disease. Therefore, we aim to determine if CYP46A1 *in vivo* ectopic expression can decrease neurotoxicity in NPC1 mice brain and improve mouse phenotype. To achieve our goal, we decided to use a recently characterized NPC mouse model that has the knock-in of the NPC1I1061T most prevalent mutation, encoding a misfolded protein. This Npc1$^{tm(I1061T)}$ mouse model faithfully recapitulates human NPC1 disease, with decreased motor coordination, brain and particularly cerebellar lesions leading to Purkinje cell death, dendritic and axonal abnormalities, lipid storage and premature death.

Initially, we had planned to use two stereotaxic injections in the cerebellar vermis with the AAVrh10-GFP or -CYP46A1 vectors that have been widely used by Cartier's lab. Nevertheless, in order to pursue a more clinically effective gene therapy approach, we have used the newly developed AAVPHPeB.HA. vector, that can cross the BBB, and therefore can be injected in the retro-orbital region, without the need for the invasive form of surgical intervention, which is the stereotaxic injection.

Wild-type mice received a retro-orbital injection with a dose of $5x10^{11}$ vg (viral genomes) of AAVPHPeB.HA.GFP (WT-GFP) vector, while Npc1$^{tm(I1061T)}$ mice received the same dose of AAVPHPeB.HA.GFP (NPC-GFP) or AAVPHPeB.HA.CYP46A1 (NPC-CYP). Mice were injected at day 35 and sacrificed at week 12.

In order to confirm efficient delivery of viral vector to the cerebellum, total protein extracts were prepared from WT-GFP, NPC-GFP and NPC-CYP cerebellum, and subjected to Western Blot analysis (Fig. 3B). We confirmed that cerebellar tissues from Npc1$^{tm(I1061T)}$ mice have decreased NPC1 protein accumulation. Moreover, a consistent and expected increase in the levels of CYP46A1 protein was observed in NPC-CYP mice. Furthermore, AAV-delivery to the

cerebellum is clearly shown by GFP expression in Purkinje neurons of the cerebellum both in WT-GFP and NPC-GFP mice (Fig. 3A).

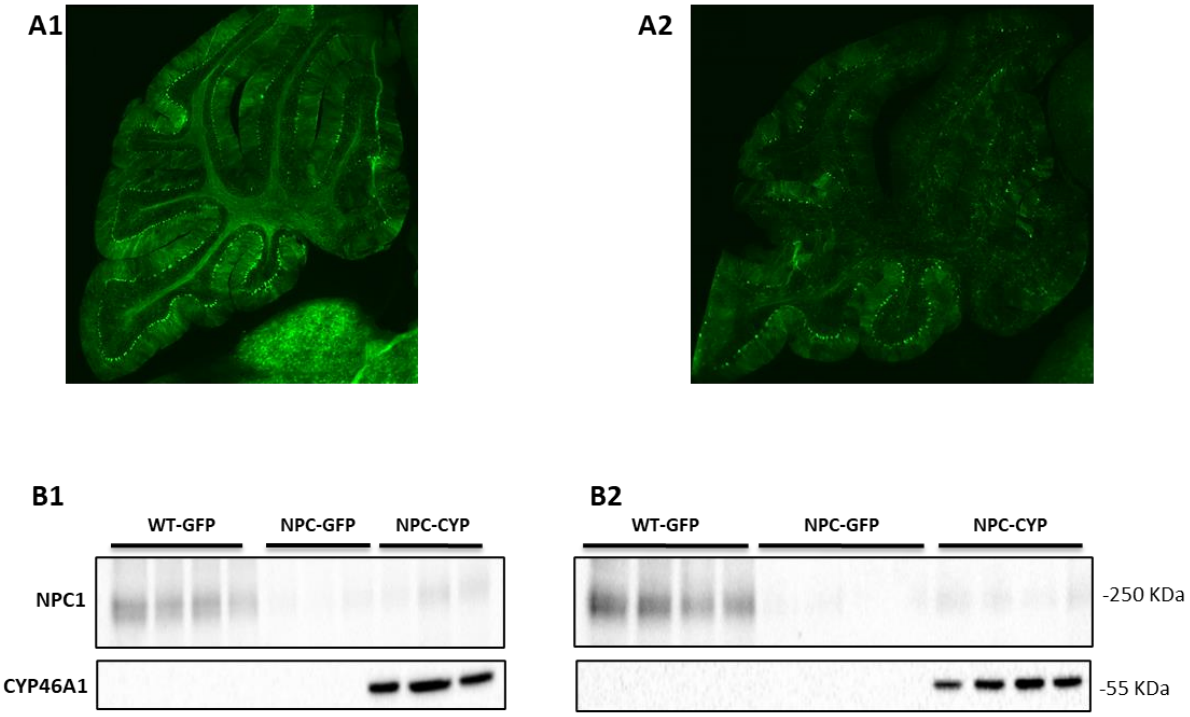

Figure 3- Expression levels of NPC1 and CYP46A1 proteins in mice cerebellum*. Wild-type mice received a retro-orbital injection with a dose of 5x10^{11} vg (viral genomes) of AAVPHPeB.HA.GFP (WT-GFP) vector, while Npc1$^{tm(I1061T)}$ mice received the same dose of AAVPHPeB.HA.GFP (NPC-GFP) or AAVPHPeB.HA.CYP46A1 (NPC-CYP). Mice were injected at day 35 and sacrificed at 12 weeks of age. AVV-mediated GFP expression in WT (A1) and NPC (A2) mouse cerebellum. Western Blot analysis of NPC1 and CYP46A1 in male (B1) and female (B2) mice cerebellum.*

NPC-GFP mice have significantly lower body weight compared with their WT littermates (Fig. 4A), and growth curves begin to diverge at 9 weeks, revealing progressive weight loss during later stages of disease. Surprisingly, female NPC-CYP mice have a significant decrease in body weight when compared with WT-GFP from week 7 onward. At 12 weeks of age, there is a significant decrease of about 25% in body weight in both male and female mice when compared with WT mice. There are no statistic significant differences between NPC-GFP and NPC-CYP animals.

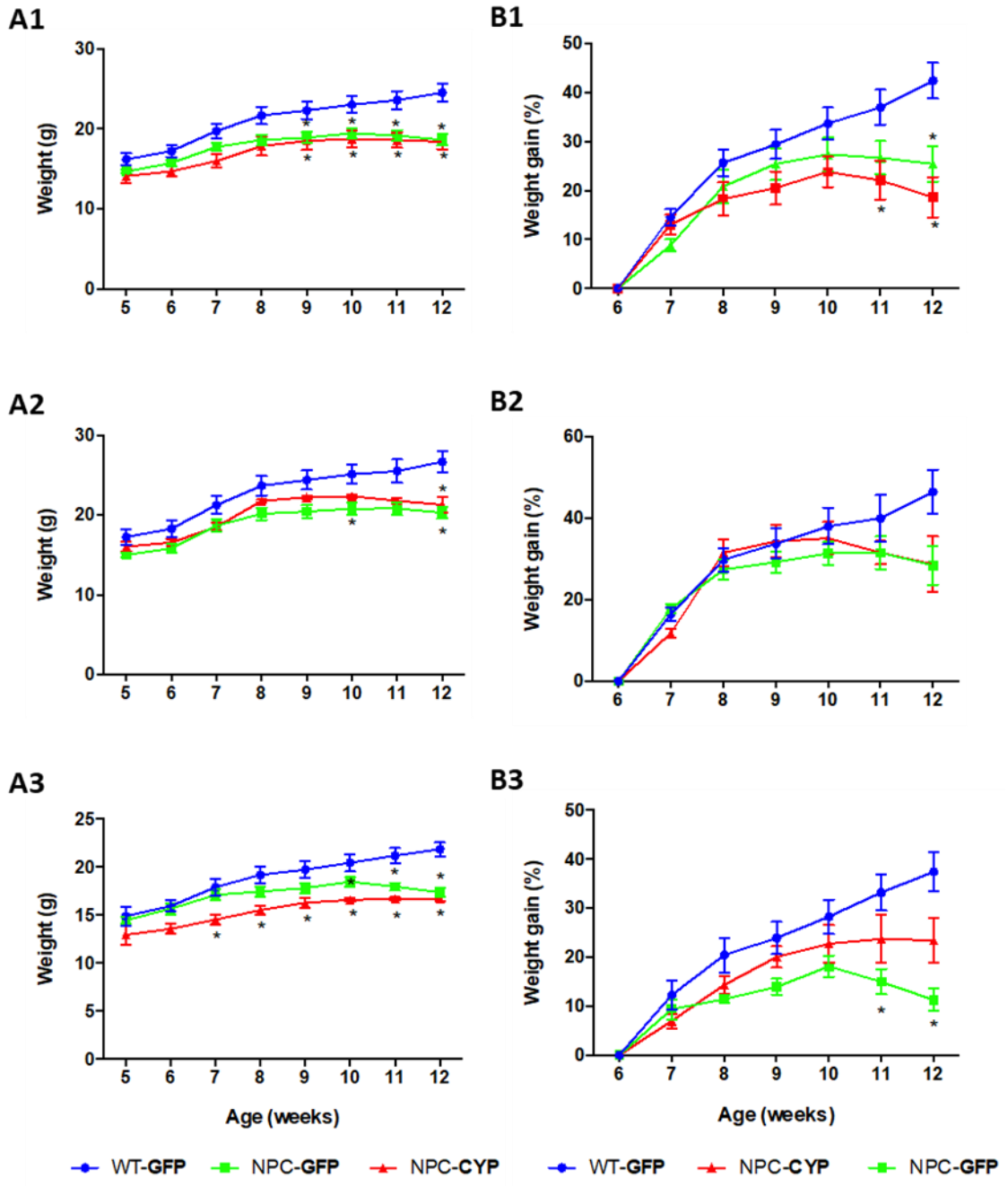

Figure 4- Animal weight over time. *Wild-type mice received a retro-orbital injection with a dose of $5x10^{11}$ vg (viral genomes) of AAVPHPeB.HA.GFP (WT-GFP) vector, while $Npc1^{tm(I1061T)}$ mice received the same dose of AAVPHPeB.HA.GFP (NPC-GFP) or AAVPHPeB.HA.CYP46A1 (NPC-CYP). Mice were injected at day 35 and weighted weekly until 12 weeks of age. Weight of all (A1), males (A2) and females (A3,) respectively. Weight gain in % in relation to 6-week-old weight of all (B1), males (B2) and females (B3), respectively. ANOVA one-way tests were performed followed by Tukey's multiple comparisons test. (*p<0.05 vs WT-GFP).*

When analysing the weight gain variation in relation to 6-week-old body weight, we can observe that while NPC-GFP female mice show a significantly decrease of the percentage of weight gain from 10 weeks onwards, this is not the case for NPC-CYP females. Indeed, NPC-CYP female mice continue to have a positive increment of approximately 23% in body weight, while NPC-

GFP females start losing weight, as shown by a decrease in gain weight from 18.1% to 11.2%, from week 10 to week 12 (Fig. 4B3). This difference was not observed in male mice.

4.2. Effect of CYP46A1 ectopic expression in neurological hallmarks of NPC disease

In NPC patients, the severe loss of Purkinje cells is one of the most evident hallmarks in the disease [63]. In order to assess Purkinje cell loss in the cerebellum, mice parasagittal brain sections were stained with cresyl violet, allowing the visualization and quantification of Purkinje cells within the three experimental groups studied (WT-GFP, NPC-GPF, NPC-CYP) (Fig. 5). NPC-GFP mice and NPC-CYP mice showed a significant decrease in the number of Purkinje cells when compared to WT-GFP littermates, mainly in the anterior zone (lobes I-V) and central zone (lobe VI+VII) of the cerebellum and in lobe VIII. As expected, cell degeneration was also observed in lobes IX-X, but to a lesser extent, since it consists of the region of the cerebellum that is usually preserved in the late-stage of the disease [93]. No striking differences were observed in Purkinje cell death between NPC-GFP and NPC-CYP animals.

A similar profile was observed in the thickness of the molecular layer. When compared with their WT-GFP littermates, NPC-GFP and NPC-CYP mice show a significant decrease in the thickness of the molecular layer in cerebellar lobes I-VIII. No significant differences were observed between NPC-GFP and NPC-CYP mice in this area, with the exception of lobes VI-VII, where CYP46A1 ectopic expression leads to a further decrease in the thickness of the molecular layer. In lobe IX the only statistical difference found was observed between WT-GFP and NPC-CYP. In lobe X, no significant differences were observed.

Regarding the thickness of the granular layer, we did not observe any significant differences between the three experimental groups.

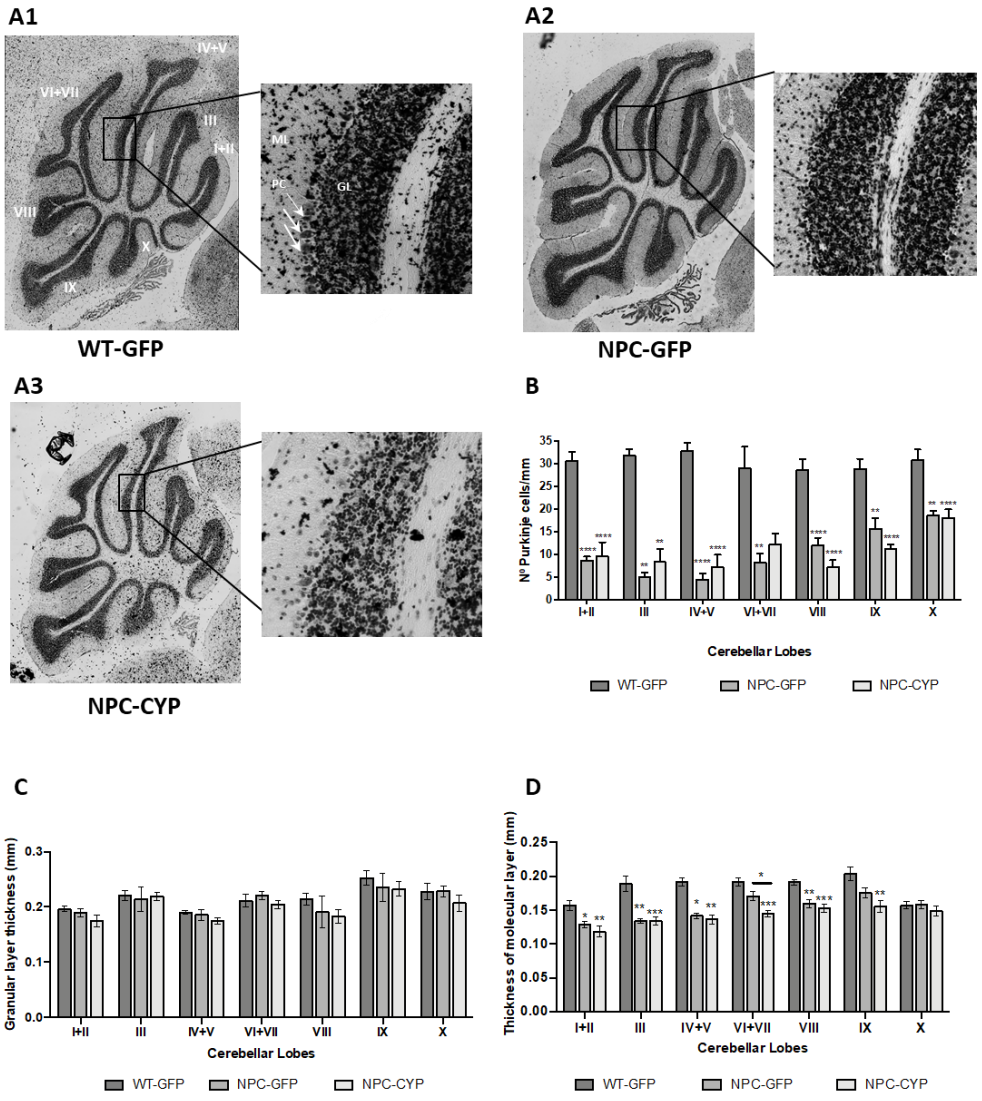

Figure 5- Cerebellar/ Purkinje cell neuropathology - Effect of CYP46A1 ectopic expression. *Wild-type mice received a retro-orbital injection with a dose of 5x10^{11} vg (viral genomes) of AAVPHPeB.HA.GFP (WT-GFP) vector, while Npc1$^{tm(I1061T)}$ mice received the same dose of AAVPHPeB.HA.GFP (NPC-GFP) or AAVPHPeB.HA.CYP46A1 (NPC-CYP). Mice were injected at day 35 and sacrificed at 12 weeks of age. Parasagittal brain sections from these animals were subjected to Cresyl Violet staining, allowing the visualization of Purkinje cells in the cerebellum of WT-GFP (A1), NPC-GFP (A2) and NPC-CYP (A3). Purkinje cells (PC) were counted and the length of the Purkinje cells layer was measured in each cerebellar lobe, allowing the determination of the Purkinje cell counts (B). The thickness of the granular layer (GL) and molecular layer (ML) are presented in panels C) and D), respectively. Data are presented as mean ± standard error of mean (SEM). ANOVA one-way tests were performed followed by Tukey's multiple comparisons test (*p<0.05, **p<0.01, ***p<0.001, ****p<0.0001 vs WT-GFP).*

4.3. Effect of CYP46A1 ectopic expression in Npc1$^{tm(I1061T)}$ mice motor function

We further examined the effect of CYP46A1 ectopic expression on the neurological disease progression in the mice using rotarod and catwalk gait analysis, which has been previously validated in NPC1 mouse models [94, 95]. Motor function tests were performed weekly from week 6 to week 12.

As far as motor symptoms are concerned at 6 weeks of age we could observe the onset of a visible resting tremor in some Npc1$^{tm(I1061T)}$ mice, and by 10 weeks, NPC-GFP mice are no longer able to maintain balance on a rotating rod, a test used to assess motor coordination. Mice were tested in a constant 10 rpm rotating drum in two consecutive days, and in Figure 6 the best performance is presented for each time point. The data shown is the sum of the time spend on the rotarod in three consecutive attempts, of a maximum of 180 seconds per attempt.

WT-GFP animals were able to maintain their balance on the rotating drum throughout the studied period. NPC-GFP and NPC-CYP animals show a significant decrease in rotarod retention time over time, from an average of 403 and 314 seconds on week 6, to approximately 16 and 22 seconds on week 12, respectively. Surprisingly, NPC-CYP males start to show a decrease in rotarod retention time as early as 6 weeks, which is significantly different from NPC-GFP male mice retention time (Fig. 6). Indeed, while male WT-GFP and NPC-GFP mice, shown a retention time superior to 400 seconds until 8 weeks of age, NPC-CYP mice at week 6 were unable to maintain balance on a rotating rod for more than 200 seconds. At 10 weeks, we could no longer observe differences in retention time between NPC-GFP and NPC-CYP animals.

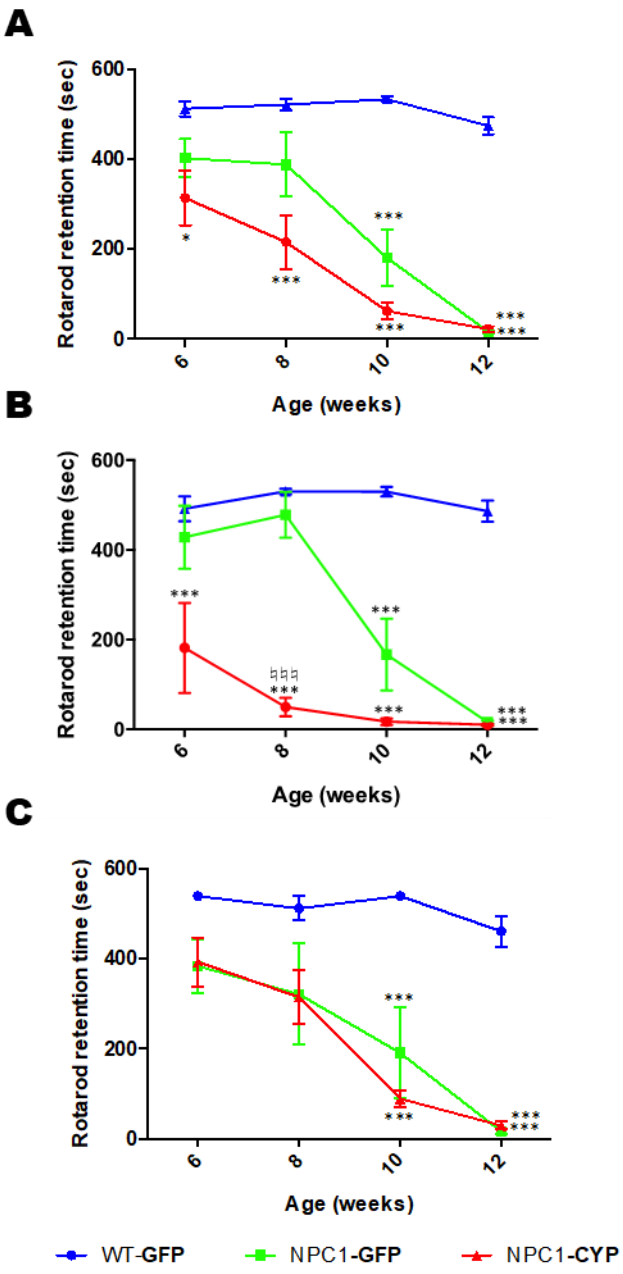

Figure 6- Motor function evaluation using the rotarod test. *$Npc1^{+/+}$ mice were injected with AAVPHPeB.HA.GFP (WT-GFP) vector, $Npc1^{tm(I1061T)}$ mice were injected with AAV-GFP (NPC-GFP) or AAVPHPeB.HA.CYP46A1 vectors (NPC-CYP) at day 35 and subjected to motor tests every two weeks, from weeks 6 until week 12. Mice were tested in a constant 10 rpm rotating drum in two consecutive days, best performance is presented for each time point. Data are shown as the sum of the time spend on the rotarod for 3 consecutive attempts, of a maximum of 180 seconds per attempt. A) all, B) male; C) female. ANOVA one-way tests were performed followed by Tukey's multiple comparisons test. (*p<0.05, ***p<0.001 vs WT-GFP; ♯♯♯p<0.001 vs NPC-GFP).*

For determination of walking speed and gait analysis, mice were placed on a transparent catwalk and their locomotion was videotaped. Analysis of the videos allowed calculating the average walking speed (Fig. 7) and the stride length (Fig. 8).

At Figure 7, we can observe that at 8 weeks of age, there are still no significant differences in average walking speed between mice from the three experimental groups, while at week 12, NPC-GFP and NPC-CYP mice show a significant decrease in average walking speed when compared with WT-GFP littermates, and with the average speed observed at 8 weeks of age. Indeed, NPC-GFP and NPC-CYP mice take longer time to cross the catwalk, registering a significantly decrease in velocity from week 8 to 12, of about 45% and 40%, respectively. No significant differences were observed between NPC-GFP and NPC-CYP at week 12.

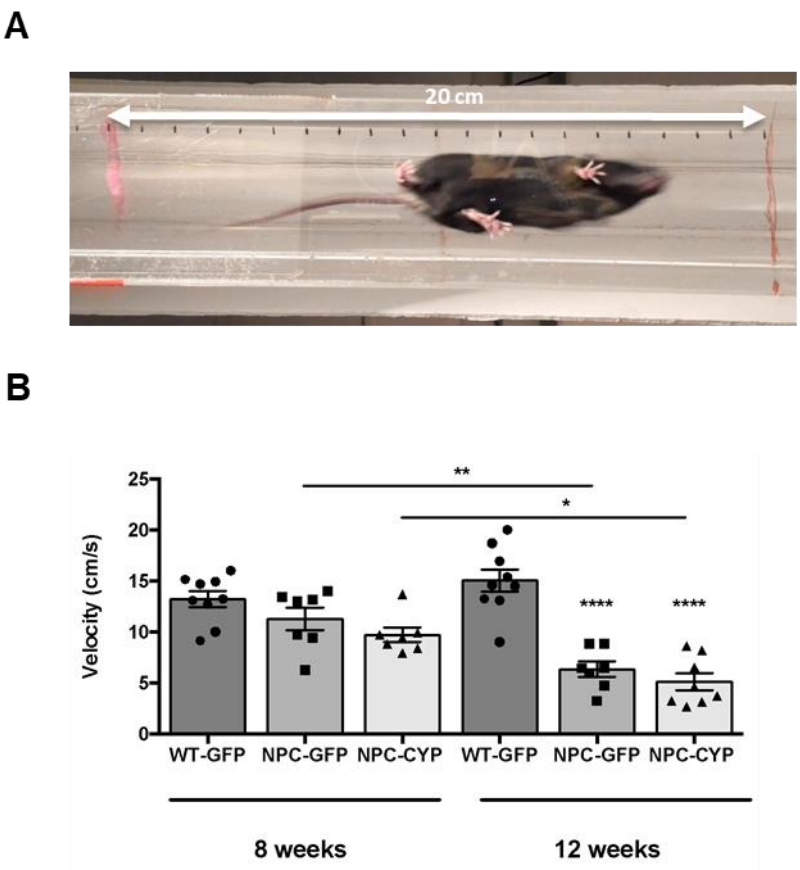

Figure 7- Locomotor function analysis - Effect of CYP46A1 ectopic expression on average walking speed. *Wild-type mice received a retro-orbital injection with a dose of $5x10^{11}$ vg (viral genomes) of AAVPHPeB.HA.GFP (WT-GFP) vector, while $Npc1^{tm(I1061T)}$ mice received the same dose of AAVPHPeB.HA.GFP (NPC-GFP) or AAVPHPeB.HA.CYP46A1 (NPC-CYP). Mice were injected at day 35 and subjected to the Catwalk analysis at week 8 and week 12. A) Each animal was placed individually in a transparent platform, where it was allowed to move freely for a maximum of 4 minutes. Animal locomotion was recorded allowing the determination of the average walking speed. Data obtained from a maximum of three runs was used to determine the average walking speed used to cross a 20 cm catwalk. B) Data are presented as mean ± standard error of mean (SEM). ANOVA one-way tests were performed followed by Tukey's multiple comparisons test (*p<0.05, **p<0.01, ****p<0.0001 vs WT-GFP).*

Gait analysis results for left and right hind and forelimbs stride length are shown in Figure 8. At 8 weeks of age, there is already a statistically significant decrease in stride length for the left hindlimb in NPC-CYP mice (Fig. 8B1), when compared with WT-GFP littermates. This decrease is still not observed for NPC-GFP. At 12 weeks of age both NPC-GFP and NPC-CYP mice show a significant decrease in left hindlimb stride length, and NPC-GFP mice also show a deterioration of coordination during movement when compared with 8 weeks of age. There are no significant differences between NPC-GFP and NPC-CYP animals at this age. A similar profile was observed for right hindlimb stride length (Fig. 8B2), and for left and right forelimbs stride length (Fig. 8B3 and B4).

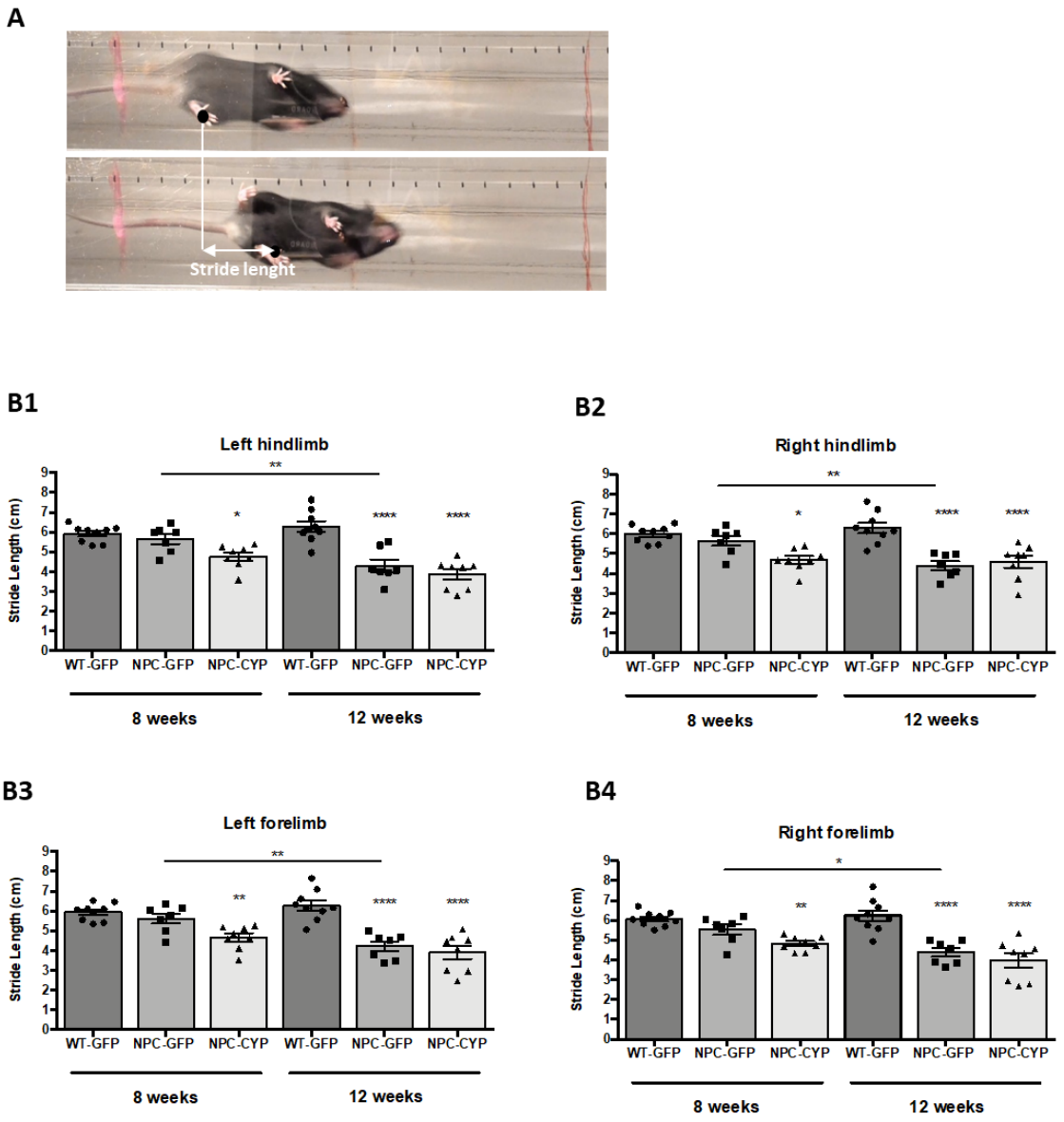

Figure 8- Locomotor function analysis - Effect of CYP46A1 ectopic expression on stride length. *Wild-type mice received a retro-orbital injection with a dose of 5x10^{11} vg (viral genomes) of AAVPHPeB.HA.GFP (WT-GFP) vector, while Npc1$^{tm(I1061T)}$ mice received the same dose of*

*AAVPHPeB.HA.GFP (NPC-GFP) or AAVPHPeB.HA.CYP46A1 (NPC-CYP). Mice were injected at day 35 and subjected to the Catwalk Gait analysis at week 8 and week 12. Each animal was placed individually in a transparent platform, where it was allowed to move freely for a maximum of 4 minutes. Animal locomotion was recorded allowing the determination of stride length as represented in A). Stride length of left (B1) and right hindlimbs (B2), and left (B3) and right forelimbs (B4) are presented as mean ± standard error of mean (SEM). ANOVA one-way tests were performed followed by Tukey's multiple comparisons test (*p<0.05, **p<0.01, ****p<0.0001 vs WT-GFP).*

Together, our findings demonstrate that CYP46A1 ectopic expression at the time of onset of NPC symptoms is not beneficial nor it induces the preservation of neurological function in $Npc1^{tm(I1061T)}$ mice.

4.4. Effect of CYP46A1 ectopic expression on gene expression in the cortex and cerebellum

As was previously mentioned Purkinje cell loss is a characteristic histological feature of NPC disease. Thus, the levels of calbindin D (Calb) mRNA were quantified in mice cortex (Fig. 9A) and cerebellum (Fig. 10A) by RT-qPCR, since this is considered a reliable marker of Purkinje cell number [96]. As expected, in the cortex no significant differences were found between WT-GFP, NPC-GFP and NPC-CYP animals. However, in the cerebellum, calbindin D mRNA levels were significantly decreased by approximately 85% in NPC-GFP when compared with WT-GFP mice. NPC-CYP animals also showed a significant decrease in calbindin D mRNA levels when compared with WT-GFP mice, and surprisingly the observed decrease of 88% was significantly higher than the one observed in the NPC-GFP group.

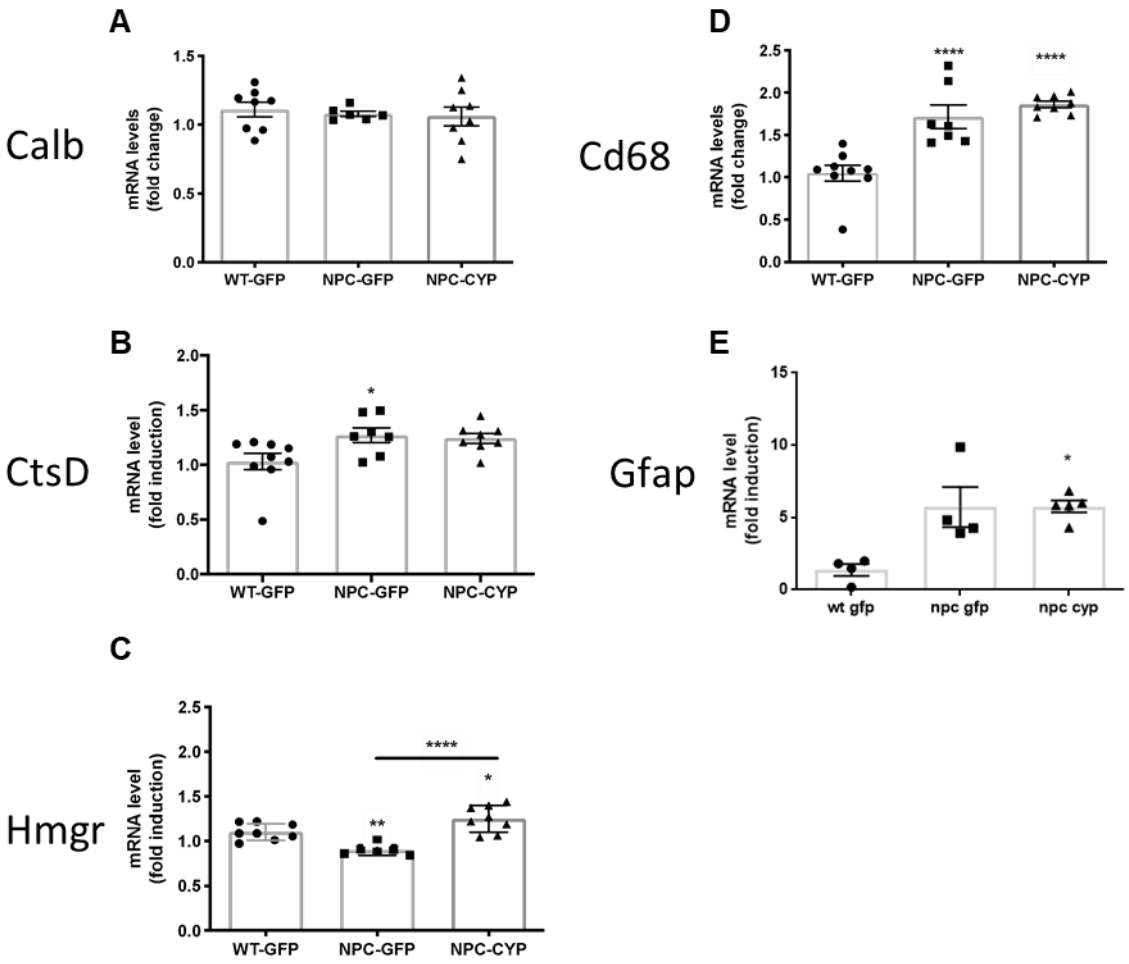

Figure 9- Effect of CYP46A1 ectopic expression on Calb, CtsD, Hmgr, Cd68 and Gfap mRNA levels in NPC mice cortex*. Wild-type mice received a retro-orbital injection with a dose of 5x10^{11} vg (viral genomes) of AAVPHPeB.HA.GFP (WT-GFP) vector, while Npc1$^{tm(I1061T)}$ mice received the same dose of AAVPHPeB.HA.GFP (NPC-GFP) or AAVPHPeB.HA.CYP46A1 (NPC-CYP). Mice were injected at day 35 and sacrificed at 12 weeks of age. mRNA was extracted from cortex samples and transcript levels were measured by RT-qPCR using RPL19 and RPL29 as reference genes. mRNA levels of Calb (A), CtsD (B), Hmgr (C), Cd68 (D) and Gfap (E) were calculated and plotted as a fold change over the average mRNA levels detected in WT-GFP mice samples and represented as mean values ± standard error of mean (SEM) (*p<0.05, **p<0.01, ****p<0.00001) (unpublished results Nunes et al.).*

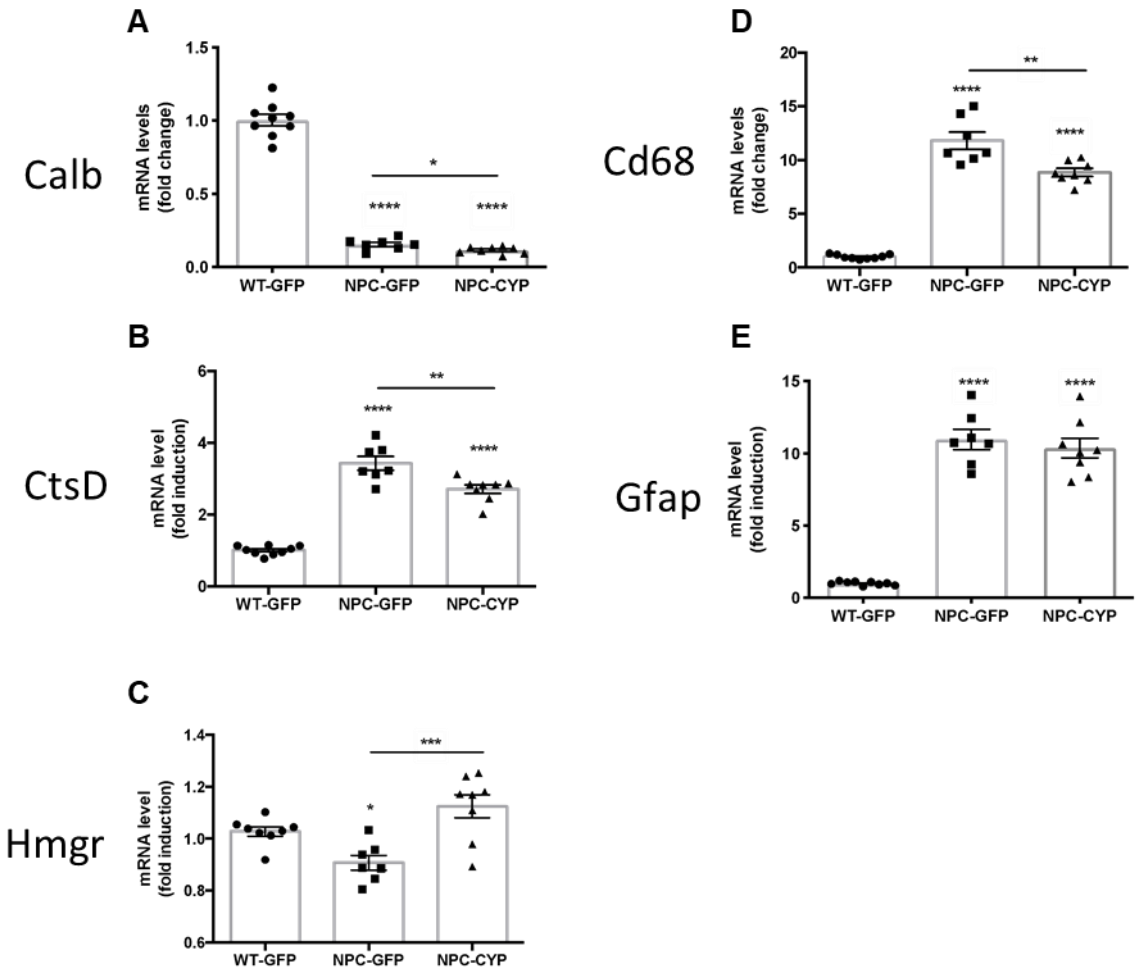

Figure 10- Effect of CYP46A1 ectopic expression on Calb, CtsD, Hmgr, Cd68 and Gfap mRNA levels in NPC mice cerebellum*. Wild-type mice received a retro-orbital injection with a dose of 5x10^{11} vg (viral genomes) of AAVPHPeB.HA.GFP (WT-GFP) vector, while Npc1$^{tm(I1061T)}$ mice received the same dose of AAVPHPeB.HA.GFP (NPC-GFP) or AAVPHPeB.HA.CYP46A1 (NPC-CYP). Mice were injected at day 35 and sacrificed at 12 weeks of age. mRNA was extracted from cerebellum samples and Calb (A), CtsD (B), Hmgr (C), Cd68 (D) and Gfap (E) transcript levels were measured by RT-qPCR using RPL19 and RPL29 as reference genes. mRNA levels were calculated and plotted as a fold change over the average mRNA levels detected in WT-GFP mice and represented as mean values ± standard error of mean (SEM) (*p<0.05, **p<0.01, ***p<0.0001, ****p<0.00001) (unpublished results Nunes et al.).*

Since lysosomal dysfunction is a key feature in NPC disease [97], we determined the mRNA levels of a lysosomal enzyme, Cathepsin D (CtsD) in mice cortex (Fig. 9B) and cerebellum (Fig. 10B). CtsD transcript levels were unaltered in the cortex of NPC-GFP and NPC-CYP animals when comparing to what was observed in WT-GFP. Regarding CtsD mRNA levels in the cerebellum, in Figure 10B we can observe a significant increase of about 3.4 fold in CtsD expression levels in NPC-GFP brain. Interestingly, although CYP46A1 ectopic expression does not restore CtsD to control levels, it induces a significant decrease of approximately 30% when compared to NPC-GFP animals.

The effect of CYP46A1 overexpression in cholesterol synthesis was also evaluated, by measuring the Hmgr mRNA levels, since HMGR is the rate-limiting enzyme in the cholesterol synthesis pathway [6]. In both cortex (Fig. 9C) and cerebellum (Fig. 10C), NPC-GFP mice present a significant decrease in Hmgr expression levels (0.8 and 0.9 fold, respectively), when comparing to WT-GFP mice. Interestingly, CYP46A1 increased expression significantly reverted this decrease, restoring levels found in WT-GFP animals.

These results suggest that CYP46A1 expression can partially normalize cholesterol homeostasis and lysosomal function in NPC mice brain.

4.5. Effect of CYP46A1 ectopic expression on neuroinflammation on the cortex and cerebellum

Neuroinflammation is a common feature of NPC disease [71]. To evaluate microgliosis and astrogliosis, we analyzed the mRNA levels of markers for microglia (Cd68) and astrocytes (Gfap). As expected, NPC-GFP mice showed significantly higher mRNA levels of Cd68 and Gfap in the cerebellum and cortex (Fig. 9 and 10), when comparing to WT-GFP animals. In the cerebellum, the mRNA levels of these genes are particularly elevated, achieving levels 11 times higher for both markers (Fig. 10D and 10E). Interestingly, CYP46A1 overexpression led to a significant decrease of about 30% in the mRNA levels of Cd68, while Gfap levels were not affected. In the cortex, the increase in Cd68 and Gfap levels is not as high as the one observed in the cerebellum (1.5 and 3-fold increase, respectively) (Fig. 9D and 9E), nevertheless, CYP46A1 expression did not affect the levels of any of the studied markers. These results indicate that glia activation can also be observed in other brain regions suggesting a broader effect in the brain that is not only confined to the cerebellum. Moreover, and more importantly, it suggests that CYP46A1 ectopic expression decreases microgliosis in NPC cerebellum.

Since our results indicate that in NPC animals injected with AAV-CYP46A1, there was a reduction of microgliosis in the cerebellum, we proceeded to study inflammation-related proteins using Western Blot analysis (Fig. 11A and 12A).

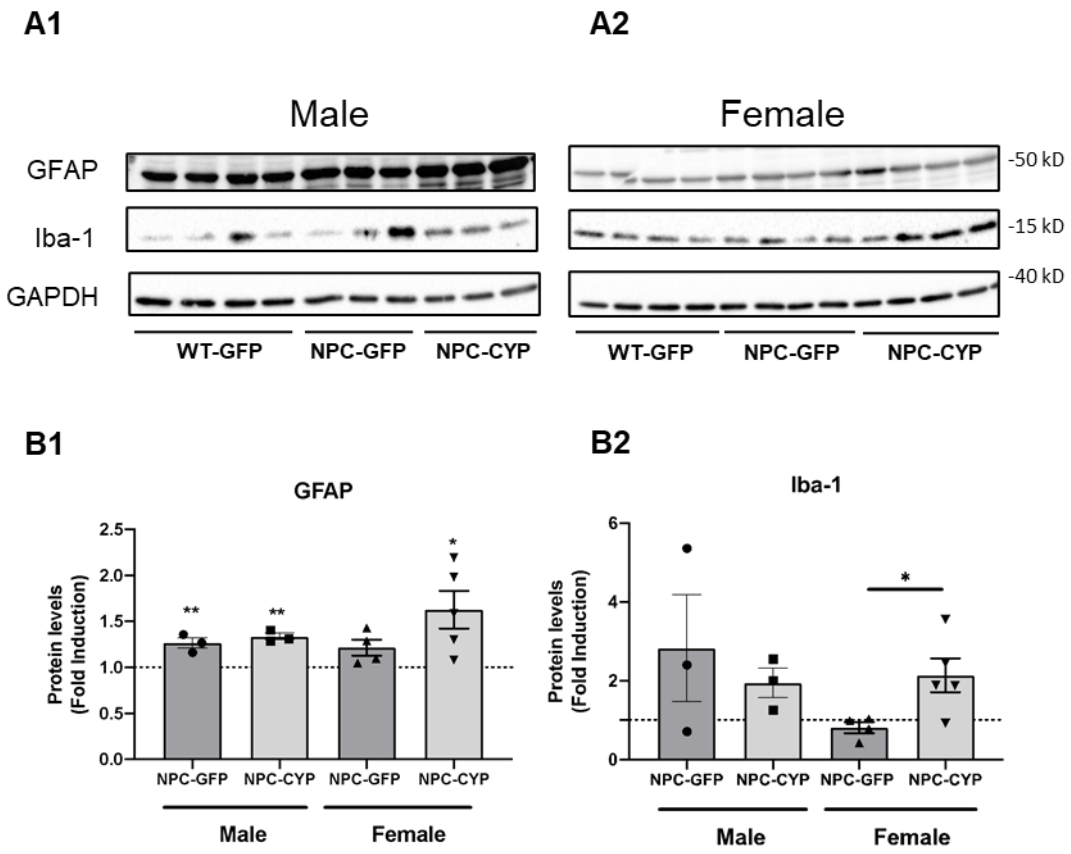

Figure 11- Effect of CYP46A1 ectopic expression on neuroinflammation in the NPC mice cortex. *Wild-type mice received a retro-orbital injection with a dose of 5x10^{11} vg (viral genomes) of AAVPHPeB.HA.GFP (WT-GFP) vector, while Npc1$^{tm(I1061T)}$ mice received the same dose of AAVPHPeB.HA.GFP (NPC-GFP) or AAVPHPeB.HA.CYP46A1 (NPC-CYP). Mice were injected at day 35 and sacrificed at 12 weeks of age. Total extracts were prepared from mice cortex samples and analyzed by Western Blot using anti-GFAP and anti-Iba-1 antibodies. GAPDH was used as loading control. The immunoblots shown are representative of the results obtained in different experiments for males (A1) and females (A2). Protein levels were calculated and plotted (B1 and B2) as fold change over the average protein levels detected in WT-GFP male and female mice, and represented as mean values ± standard error of mean (SEM) (*p<0.05, **p<0.01). [ER1]*

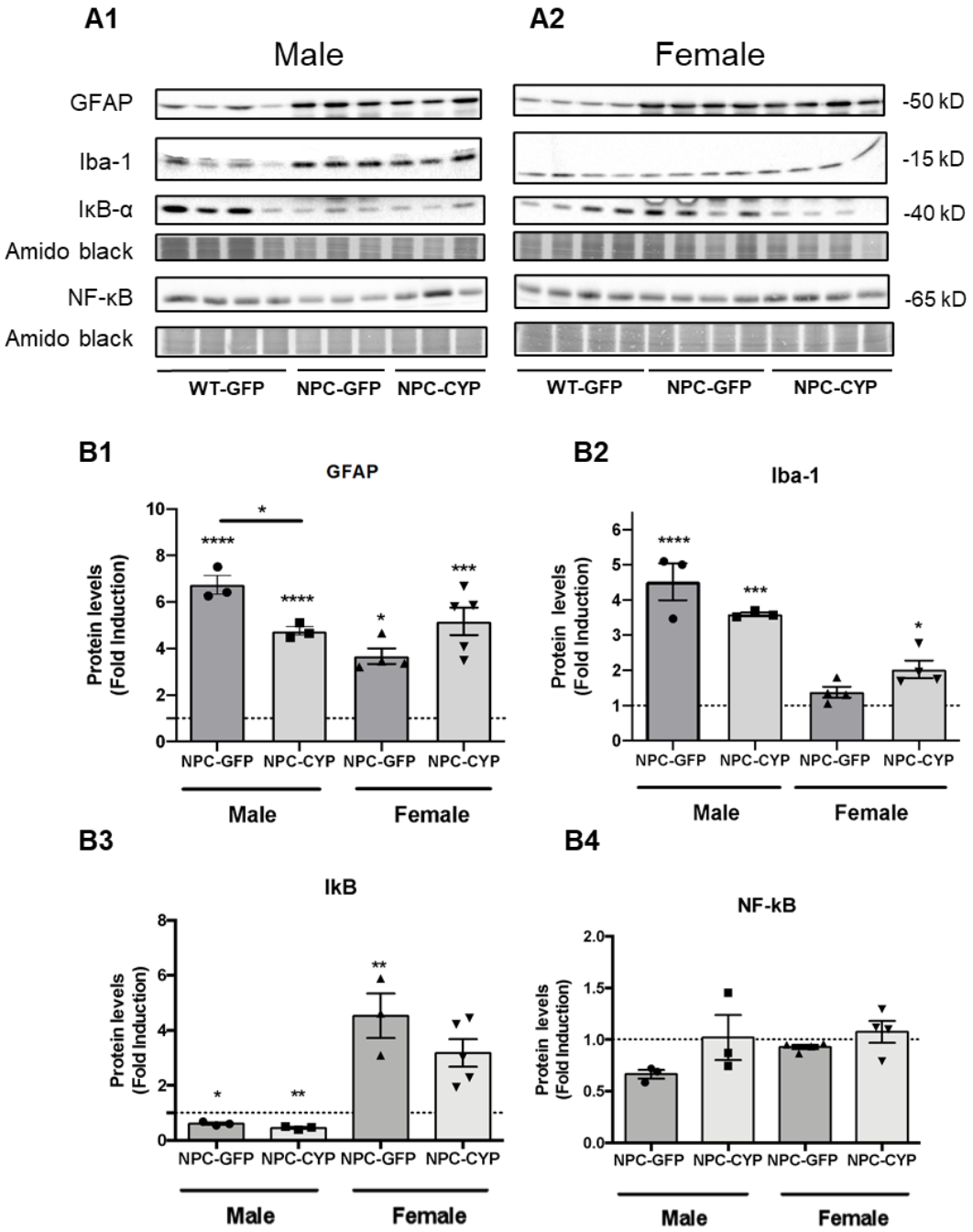

Figure 12- Effect of CYP46A1 ectopic expression on neuroinflammation in NPC mice cerebellum*. Wild-type mice received a retro-orbital injection with a dose of 5x10^{11} vg (viral genomes) of AAVPHPeB.HA.GFP (WT-GFP) vector, while Npc1$^{tm(I1061T)}$ mice received the same dose of AAVPHPeB.HA.GFP (NPC-GFP) or AAVPHPeB.HA.CYP46A1 (NPC-CYP). Mice were injected at day 35 and sacrificed at 12 weeks of age. Total extracts were prepared from mice cerebellum samples and analyzed by Western Blot using anti-GFAP, anti-Iba-1, anti-IκB-α and anti-p65 antibodies. Amido black staining was used as loading control. The immunoblots shown are representative of the results obtained in different experiments for males (A1) and females (A2). Protein levels were calculated and plotted (B1, B2, B3 and B4) as a fold change over the average protein levels detected in WT-GFP male and female mice, and represented as mean values ± standard error of mean (SEM) (*p<0.05, **p<0.01, ***p<0.0001, ****p<0.00001). [ER1]*

In contrast to what was observed at the mRNA level, we could observe some sex differences in the protein levels, and therefore the analysis of protein levels was performed independently for males and females (Figure 11 and 12).

In accordance with the results we obtained for the mRNA analysis, we observed a significant increase of 1.3 fold in GFAP protein levels in the cortex of NPC-GFP male mice, and CYP46A1 expression did not prevent this increase (Fig. 11B1). In females, we also have the same tendency; nevertheless, only NPC-CYP females showed a significant increase of 1.6 fold in GFAP levels, in comparison to those found in WT-GFP animals. Although we had observed a significant increase in Cd68 mRNA levels in the cortex, no significant differences were found in Iba-1 expression in this brain region, although NPC-CYP females have higher levels of this protein when compared to NPC-GFP female mice (Figure 11B2).

In parallel with the results obtained for the mRNA analysis, overall, we observed a higher increase in astrocytic and microglial protein markers in the cerebellum of NPC-GFP mice (Fig. 12). Indeed, we could observe in males and females a significant increase in GFAP protein levels of approximately 7 and 4 fold (Fig. 12B1), respectively. Interestingly, CYP46A1 expression led to a significant decrease in GFAP expression of about 30%, but this effect was not observed in females. When analyzing the expression levels of Iba-1, we could also observe a significant increase of about 5 fold in NPC-GFP males (Figure 12B2), but in contrary to what we had observe at the mRNA level, CYP46A1 expression did not significantly affect the expression of this marker. Surprisingly, and in complete opposition to what we had observed at the mRNA level for the microglial target gene, we could not detect a statistically significant increase in Iba-1 in the cerebellum of NPC-GFP female mice, and actually we could detect a small but significant 2 fold increase in Iba-1 levels in NPC-CYP animals.

Glia activation is usually indicative of an inflammatory environment; therefore, we decided to evaluate NF-κB and IκB-α protein levels, since this transcription factor is a major regulator of inflammation [25]. As previously mentioned, the activation of NF-κB is preceded by IκB-α degradation, which then releases NF-κB subunits to migrate into the nucleus [25] .

In male cerebellum, where we observed higher levels of astrogliosis and microgliosis, NPC-GFP and NPC-CYP mice showed a significant decrease in IκB-α protein levels (Fig. 12B3), when comparing to what was observed in WT-GFP animals (0.6 and 0.4 fold, respectively), suggesting a putative activation of NF-κB. Surprisingly, in females, there is a significant increase in IκB-α protein levels in NPC-GFP mice of about 4.5 times, and we could also observe a similar tendency in the brains of NPC-CYP females (3.2 fold increase, p=0.054) (Fig. 12B3). Western blot analysis showed no significant differences for p65 subunit of NF-κB (Fig. 12B4) in all groups tested. Since p65 levels are unchanged and IκB-α protein levels are up-regulated in the female brain, one could envision a decrease in NF-κB activation. Nevertheless, this does not seem to be the case. Indeed, results from Figure 13 demonstrate that in the cerebellum of males and females, both in NPC-GFP and NPC-CYP animals, there is a

significant increase in the mRNA levels of NF-κB target genes, IL-1α and IL-1β. Actually, the increase in IL-1α and IL-1β mRNA levels are higher in NPC-GFP females (3.9 and 16.3, respectively), than in males (1.7 and 3.9. respectively).

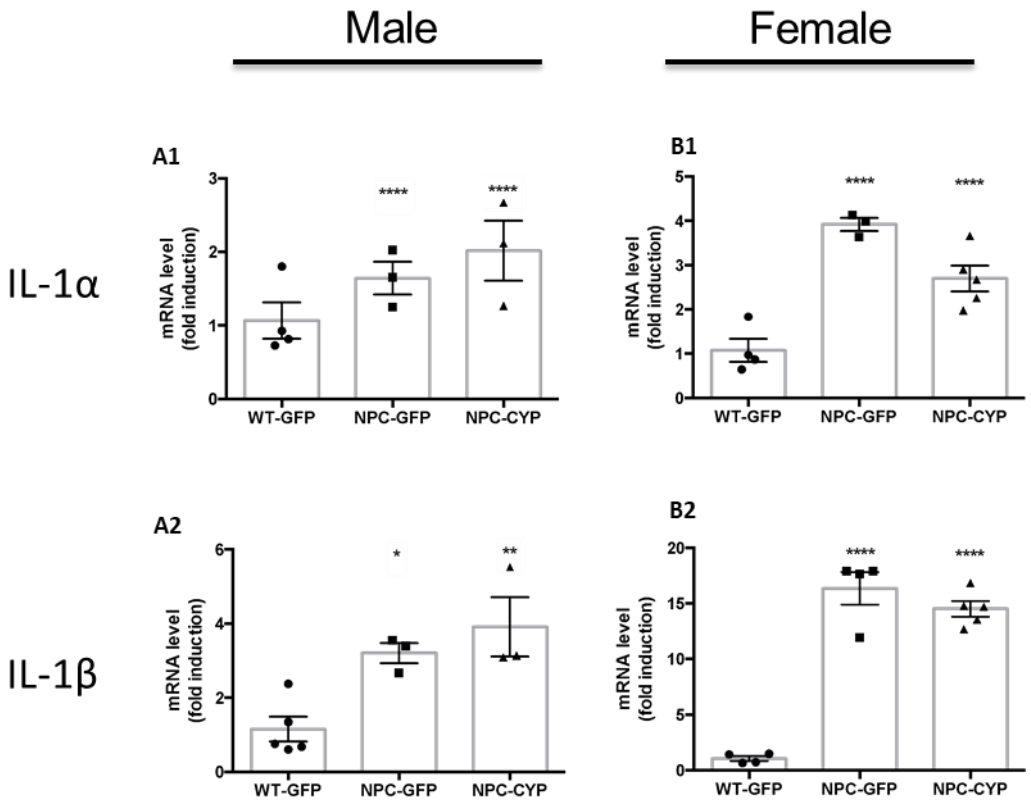

Figure 13- Effect of CYP46A1 ectopic expression on cytokines levels in NPC mice cerebellum. *Wild-type mice received a retro-orbital injection with a dose of 5x10^{11} vg (viral genomes) of AAVPHPeB.HA.GFP (WT-GFP) vector, while Npc1$^{tm(I1061T)}$ mice received the same dose of AAVPHPeB.HA.GFP (NPC-GFP) or AAVPHPeB.HA.CYP46A1 (NPC-CYP). Mice were injected at day 35 and sacrificed at 12 weeks of age. mRNA was extracted from cerebellum samples and IL-1α and IL1-β transcript levels were measured by RT-qPCR using RPL19 and RPL29 as reference genes. mRNA levels were calculated and plotted (A1 and A2, B1 and B2) as a fold change over the average mRNA levels detected in WT-GFP male and female mice, and represented as mean values ± standard error of mean (SEM) (*p<0.05, **p<0.01, ****p<0.00001) (unpublished results Nunes et al.).*

Overall, our results suggest that at least in the cerebellum of NPC male mice CYP46A1 ectopic expression decreases neuroinflammation levels.

4.6. Effect of CYP46A1 ectopic expression on autophagy in NPC disease

Since autophagy defects are also observed in NPC disease [98], we tried to quantify the levels of native and lipidated LC3 (LC3-I and LC3-II, respectively) in NPC mice brain (Fig. 14). Unfortunately, we could not detect LC3 levels in mice cerebellum. In the cortex, NPC-GFP male

and female mice showed a significantly increase of about 3 and 7 fold in LC3 II/I ratio, respectively, when compared with WT-GFP animals. Interestingly, CYP46A1 ectopic expression led to a significant 30% decrease in LC3 II/I ratio when comparing NPC-GFP and NPC-CYP females. A similar tendency was observed in males.

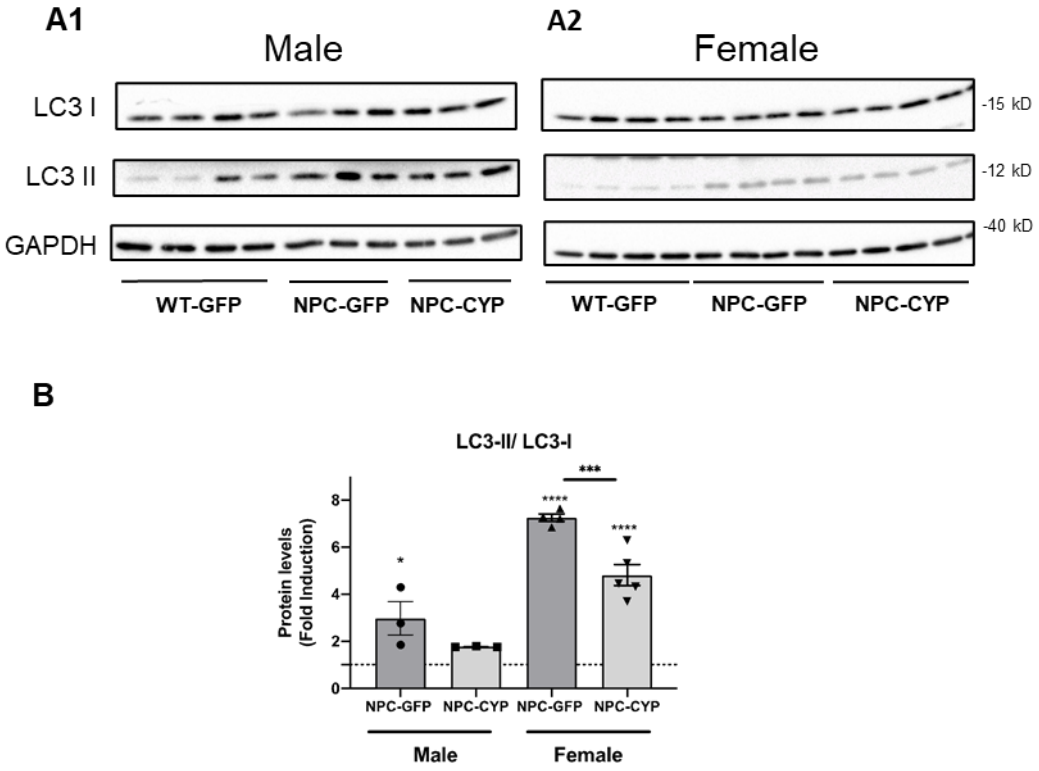

Figure 14- Effect of CYP46A1 ectopic expression on LC3-II/ LC3-I ratio in the NPC mice cortex. *Wild-type mice received a retro-orbital injection with a dose of $5x10^{11}$ vg (viral genomes) of AAVPHPeB.HA.GFP (WT-GFP) vector, while $Npc1^{tm(I1061T)}$ mice received the same dose of AAVPHPeB.HA.GFP (NPC-GFP) or AAVPHPeB.HA.CYP46A1 (NPC-CYP). Mice were injected at day 35 and sacrificed at 12 weeks of age. Total extracts were prepared from mice cortex samples and analyzed by Western Blot using an anti-LC3 antibody. GAPDH was used as loading control. The immunoblots shown are representative of the results obtained in different experiments for males (A1) and females (A2). Protein levels were calculated and plotted (B) as fold change over the average protein levels detected in WT-GFP male and female mice, and represented as mean values ± standard error of mean (SEM) (*p<0.05, ***p<0.0001, ****p<0.00001).*

These results suggest that CYP46A1 expression can partially normalize autophagy defects in NPC mice brain.

5. Discussion and future perspectives

CYP46A1 is a major player in brain cholesterol homeostasis, modulating cholesterol metabolism, synthesis and efflux [14]. Hence, it is plausible that this enzyme might play an important role in pathological contexts characterized by an imbalance in cholesterol homeostasis. This has been corroborated by the previously cited studies from the group of Natalie Cartier showing that increased expression of CYP46A1 *in vivo* is beneficial in different models of neurodegenerative disorders [46, 48]. To further test this idea, we decided to assess the effect of CYP46A1 in a model of NPC disease, a genetic lysosomal storage disorder, characterized by the accumulation of unesterified cholesterol in late endosomes/ lysosomes due to impaired egress [60, 62]. Indeed, cholesterol accumulation leads to gradual neurodegeneration, the most dominant and fatal feature of this disease [91].

Our initial results show that cholesterol levels and more importantly, cholesterol accumulation in late endosomes/ lysosomes is robustly reduced upon CYP46A1 ectopic expression in human NPC1 (I1061T) fibroblasts (Costa et al. unpublished results). This effect was also accompanied by partial normalization of the mRNA levels of several genes involved in cholesterol homeostasis and ATP levels, which were greatly deregulated in NPC1 fibroblasts. NPC1I1061T is the most common mutation found in NPC patients, which encodes a misfolded protein that has a reduced half-life, since it is targeted for proteasomal degradation [90]. It has been shown that several oxysterols and their derivatives act as pharmacological chaperones, and that binding of these compounds to NPC1I1061T corrects the localization/ maturation defect of the mutant protein [99]. Therefore, since one of the putative neuroprotective roles of CYP46A1 could depend on the increased production of 24OHC, we opted to use the $Npc1^{tm(I1061T)Dso}$ knock-in mouse model [63]. These mice exhibit less severe and delayed manifestations of NPC1 disease, including weight loss, motor coordination, Purkinje cell loss, lipid storage, and premature death, when compared to the $Npc1^{-/-}$ model [63]. Importantly, the NPC1I1061T protein produced in these mice has a reduced half-life *in vivo*, due to protein misfolding and rapid ER-associated degradation, however it can be stabilized *in vivo*, as was already exemplified by histone deacetylase inhibition [63]. To increase the levels of CYP46A1, we have used an AAV gene mediated therapy with a vector encoding CYP46A1 in $Npc1^{tm(I1061T)}$ mice, resulting in CYP46A1 ectopic expression. In order to pursue a clinically effective gene therapy approach, we opted to use the newly developed AAVPHPeB.HA.CYP46A1 vector that can cross the BBB, and therefore can be injected in the retro-orbital region, without the need for the invasive form of surgical intervention, such as the stereotaxic injection. Our results show that with this approach we obtain high levels of expression of the transgene in the cerebellum of NPC mice.

CYP46A1 ectopic expression was able to prevent weight loss in females, but the same effect was not observed in male mice. Actually, in contrary to what was initially described by

Praggastis and collaborators [63], we have observed a high heterogeneity between Npc1$^{tm(I1061T)}$ animals, which was observed upon handling, as early as 6 weeks of age. This more severe phenotype was particularly evident in males. In fact, the 3 male mice littermates that were injected with AAV-CYP vector, showed resting tremor and presented a more aggravated disease phenotype, already at week 6, a time-point when the expression of transgene is still not high (N. Cartier, personal communication). Moreover, the fact that NPC mice were injected at 5 weeks of age, instead of at 3 weeks of age, as we had previously intended, coinciding with the onset of the disease symptoms, may be one of the reasons why we could not see any amelioration in terms of Purkinje cell survival and motor function in mice overexpressing CYP46A1. The fact that some mice present earlier onset of disease symptoms, is a cofounding factor that must be taken into consideration when planning future injection protocols.

The fact that we observe extensive Purkinje cell death in the cerebellum of both NPC-GFP and NPC-CYP mice is correlated with the lack of improvement in motor function. Nevertheless, we believe that a more detailed gait analysis will give more consistent and informative information regarding the Npc1 phenotype [100]. Therefore, additionally to the stride length and average velocity determined in this work, other parameters should be measured, including step sequence, swing speed, regularity index, single support, lateral support and girdle support [100].

Although, we did not observe any benefit of CYP46A1 expression in terms of motor function and neuropathologic features, the molecular and biochemical analysis of NPC mice cerebellar samples has showed that CYP46A1 can ameliorate important pathological characteristics of the disease. Importantly, CYP46A1 expression could revert the decrease in Hgmr mRNA levels observed in NPC mice, suggesting that CYP46A1 can revert defects on cholesterol homeostasis. A decrease in the mRNA levels of genes involved in cholesterol synthesis has already been described for other NPC mice models [101]. Moreover, unpublished work from our group reveals that CYP46A1 restores the mRNA levels of other genes involved in cholesterol synthesis which are decreased in NPC mice cerebellum, such as HMG-CoA synthase (HMGS), SREBP2 and LDLR, while it downregulates genes that are upregulated in NPC mice brain, such as ATP binding cassette transporter A1 (ABCA1) and acetyl-CoA acetyltransferase 1 (ACAT1) (Nunes et al., unpublished results). Importantly, in the near future we will have to perform filipin staining in cerebellum slices, in order to conclude if there is a redistribution of cholesterol within the cells. Concomitantly, with the restoration of cholesterol homeostasis, we could observe a down-regulation of CtsD in the cerebellum of AAV-CYP injected Npc1$^{tm(I1061T)}$ mice, suggesting that CYP46A1 can partially correct lysosomal dysfunction observed in NPC mice [97]. Lysosomal dysfunction is often associated with defects in autophagy. Indeed, it has been shown that defective autophagy in NPC disease is associated with cholesterol accumulation, where the maturation of autophagosomes is impaired because of defective amphisome formation caused by failure in the SNARE machinery, whereas the lysosomal proteolytic function remains unaffected [70]. To determine the status of autophagic activity in brains of NPC-GFP mice, levels of LC3, were assessed in the cortex by immunoblotting. LC3 is modified via a

ubiquitination-like system; LC3 is first cleaved in its carboxyl terminal and becomes LC3-I, which is further modified by autophagy related 7 (Atg7) and Atg3 into a membrane-bound form, LC3-II [102]. Modification of LC3 is essential for the formation of autophagosomes; thus LC3-II has been widely used as an autophagosomal marker. Our results show an increase in the LC3-II/ LC3-I ratio, that is probably not due to increased autophagosome synthesis but rather is caused by impaired degradation of autophagosomes. Interestingly, the LC3-II/LC3-I ratio decreased in the cortex of AAV-CYP46A1 injected $Npc1^{tm(I1061T)}$ mice, indicating that CYP46A1 expression can partially normalize autophagy defects in NPC mice brain. Therefore, it would be very interesting to determine the colocalization of LC3+ and Rab7+ vesicles in NPC-CYP *versus* NPC-GFP mice. Interestingly, we have increased prenylation and activation of small guanosine triphosphate-binding proteins (sGTPases) induced by overexpression of CYP46A1 [103]. These sGTPases, such as Rab7, are involved in various processes implicated in cellular trafficking, including construction of the autophagosome and its fusion with the lysosome. Moreover, since we have already observed a similar effect of CYP46A1 in cellular models of NPC disease, it would be interesting to inhibit prenyltransferases activity, and determine if the effect of CYP46A1 expression on LC3-II levels is compromised. The down-regulation of CtsD and LC3-II suggests an improvement of the cellular trafficking when cholesterol homeostasis is re-established [97, 104], however, this was not sufficient to promote Purkinje cell survival. Nonetheless, the severe Purkinje cell loss observed could be caused by the retention of other lipids, such as sphingolipids, since it has been previously demonstrated that Purkinje cell loss is also related to accumulation of sphingolipids and, in particular, sphingosine [105]. Therefore, in the future it would be interesting to do a thorough lipidomic analysis.

Another important aspect is that our results suggest that overexpression of CYP46A1 is involved in the reduction of neuroinflammation in the cerebellum. NPC mice show increased astrogliosis and microgliosis in both the cortex and the cerebellum, being this increase more exacerbated in the cerebellum, as expected. Specifically, in male mice we can observe a decrease in Cd68 mRNA levels, and a decrease in GFAP protein levels after CYP46A1 expression. In females the results obtained are more difficult to interpret because we do not have a correlation between what we observe at the mRNA and the protein level. Our results are, so far, very preliminary, and a thorough characterization of other anti- and pro-inflammatory markers is needed. Indeed, we will need to make a distinction between microglia and macrophages, because CD68 is a common marker for both types of cells. We could separate microglia from other cells of the periphery and CNS by preparation of a single-cell suspension followed by fluorescence-activated cell sorting based on the membrane expression of Cluster of Differentiation 11b ($CD11b^{high}$) and Cluster of Differentiation 45 ($CD45^{low/int}$). Although, recent studies have led to the abandonment of the static M1-M2 concept of microglial phenotypes [106] and macrophage activation [107] states, and point toward the adaption of a so-called multidimensional concept, it would be interesting and easy to determine the mRNA levels of homeostatic microglial gene signature which is normally downregulated during neurological diseases, such as spalt like transcription factor 1 *(Sall1),* Spi-1 proto-oncogene *(Pu.1),*

transmembrane protein 119 *(Tmem119),* chemokine (C-X3-C motif) receptor 1 *(Cx3cr1),* and purinergic receptor P2Y, G-protein coupled 12/13 (*P2ry12/13)* and upregulated genes such as apolipoprotein E *(Apoe)* and triggering receptor expressed on myeloid cells 2 *(Trem2)* [108], and to see the effect of CYP46A1. Importantly, sex-specific transcriptomic signatures are found when comparing adult male and female mice. A higher gene expression level of inflammatory response genes, such as C-C motif chemokine 2 *(Ccl2), Tnf*, interferon regulatory factor 1 *(Irf1),* C-X-C motif chemokine 10 *(Cxcl10),* and *Il-1β* is found in female mice, indicating a more immune-activated state of female microglia. In addition, homeostatic microglial signature genes are also differentially expressed in male and female mouse microglia [108]. This also must be taken into consideration, after we make a more detailed characterization of microglia activation on NPC mice.

The role of CYP46A1 in the neuroinflammation reduction can be either an indirect effect of the re-establishment of cholesterol homeostasis, or a direct effect due to the activation of LXR. Surprisingly, some reports have suggested, however, that substantial overproduction of 24OHC by CYP46A1 overexpression was unable to affect LXR activation in the brain or liver [109]. Therefore, firstly we will need to measure 24OHC levels in brain and in the plasma of NPC-GFP and NPC-CYP mice. Afterwards, we will have to characterize LXR target genes response. The mechanisms underlying the repressive activity of LXR on inflammatory genes is still controversial and have been attributed to cholesterol efflux or to transrepression of NF-κB and activator protein-1 (AP-1) activity. More recently, it has been suggested that although cholesterol efflux contributes to LXR repression, the direct repressive functions of LXR are independent of AP-1, and that LXR reduces chromatin accessibility in *cis* at inflammatory gene enhancers containing LXR binding sites [17]. Therefore, it would be interesting to determine chromatin accessibility, by analysing activating histone marks, acetylation of histone H3 on lysine 27 (H3K27ac) or histone H3 lysine 4 dimethylation (H3K4me2), by chromatin immunoprecipitation, at inflammatory gene enhancers containing LXR binding sites, in NPC-GFP and NPC-CYP mice.

To better understand alteration in NF-κB pathway activation in the cerebellum, which is supported by the increased GFAP and Iba-1 expression in astrocytes and microglia, respectively, and also increased expression of IL-1α and IL-1β, we should pursue with quantification of the phospho-IκB-α/ IκB-α ratio, quantification of p65, and/or other NF-κB subunits, in the nucleus by Western Blot analysis using nuclear extracts, or immunofluorescence analysis to determine if NF-κB is translocated to the nucleus.

In summary, although our results are not what we initially anticipated, since injection of an AAV vector encoding CYP46A1 did not result in overall improvement of the NPC disease phenotype, the molecular and biochemical analysis revealed promising results, since CYP46A1 ectopic expression is able to ameliorate important features of NPC disease, such as cholesterol homeostasis, lysosomal function and neuroinflammation. These results suggest that an earlier intervention, at an earlier age, before the onset of the disease can open a new therapeutic

avenue for this disease. Moreover, since this research approach is to target a molecular pathway that mediates neuroprotection in different models of neurodegeneration, our results can have a broaden impact on other neurodegenerative disorders with altered brain cholesterol and can accelerate translation into potential therapies for improving human health in an area where no significant therapeutic advances have been made.

References

[1] J. M. Dietschy, “Central nervous system: Cholesterol turnover, brain development and neurodegeneration,” *Biol. Chem.*, vol. 390, no. 4, pp. 287–293, 2009, doi: 10.1515/BC.2009.035.

[2] L. C and S. M, “Cholesterol Homeostasis Imbalance and Brain Functioning: Neurological Disorders and Behavioral Consequences,” *J. Neurol. Neurol. Disord.*, vol. 1, no. 1, pp. 1–14, 2014, doi: 10.15744/2454-4981.1.101.

[3] A. Zampelas and E. Magriplis, “New Insights into Cholesterol Functions: A Friend or an Enemy?,” *Nutrients*, vol. 11, no. 7, 2019, doi: 10.3390/nu11071645.

[4] Z. Korade, “Lipid rafts, cholesterol, and the brain,” *Bone*, vol. 23, no. 1, pp. 1–7, 2008, doi: 10.1038/jid.2014.371.

[5] I. L. Shapiro, J. A. Jastremsky, D. A. Eggen, and D. Kritchevsky, “Cholesterol metabolism in the brain,” *Lipids*, vol. 3, no. 2, pp. 136–142, 1968, doi: 10.1007/BF02531730.

[6] F. Arenas, C. Garcia-Ruiz, and J. C. Fernandez-Checa, “Intracellular cholesterol trafficking and impact in neurodegeneration,” *Front. Mol. Neurosci.*, vol. 10, no. November, 2017, doi: 10.3389/fnmol.2017.00382.

[7] J. M. Dietschy and S. D. Turley, “Cholesterol metabolism in the central nervous system during early development and in the mature animal,” *J. Lipid Res.*, vol. 45, no. 8, pp. 1375–1397, 2004, doi: 10.1194/jlr.R400004-JLR200.

[8] J. Egawa, M. L. Pearn, B. P. Lemkuil, P. M. Patel, and B. P. Head, “Membrane lipid rafts and neurobiology: age-related changes in membrane lipids and loss of neuronal function,” *J. Physiol.*, vol. 594, no. 16, pp. 4565–4579, 2016, doi: 10.1113/JP270590.

[9] J. Chen, X. Zhang, H. Kusumo, L. G. Costa, and M. Guizzetti, “Cholesterol efflux is differentially regulated in neurons and astrocytes: Implications for brain cholesterol homeostasis,” *Biochim. Biophys. Acta - Mol. Cell Biol. Lipids*, vol. 1831, no. 2, pp. 263–275, 2013, doi: 10.1016/j.bbalip.2012.09.007.

[10] T. C. Genaro-Mattos, A. Anderson, L. B. Allen, Z. Korade, and K. Mirnics, “Cholesterol Biosynthesis and Uptake in Developing Neurons,” *ACS Chem Neurosci.*, vol. 10, no. 8, pp. 3671–3681, 2019, doi: 10.1021/acschemneuro.9b00248.Cholesterol.

[11] F. Djelti *et al.*, “CYP46A1 inhibition, brain cholesterol accumulation and neurodegeneration pave the way for Alzheimer’s disease,” *Brain*, vol. 138, no. 8, pp. 2383–2398, 2015, doi: 10.1093/brain/awv166.

[12] J. E. Vance, “Dysregulation of cholesterol balance in the brain: Contribution to neurodegenerative diseases,” *DMM Dis. Model. Mech.*, vol. 5, no. 6, pp. 746–755, 2012, doi: 10.1242/dmm.010124.

[13] V. Howe *et al.*, “Cholesterol homeostasis: How do cells sense sterol excess?,” *Chem. Phys. Lipids*, vol. 199, pp. 170–178, 2016, doi: 10.1016/j.chemphyslip.2016.02.011.

[14] D. W. Russell, R. W. Halford, D. M. O. Ramirez, R. Shah, and T. Kotti, “Cholesterol 24-Hydroxylase: An Enzyme of Cholesterol Turnover in the Brain,” *Annu. Rev. Biochem.*, vol. 78, no. 1, pp. 1017–1040, 2009, doi: 10.1146/annurev.biochem.78.072407.103859.

[15] R. Courtney and G. E. Landreth, “LXR Regulation of Brain Cholesterol: From Development to Disease,” *Trends Endocrinol. Metab.*, vol. 27, no. 6, pp. 404–414, 2016, doi: 10.1016/j.tem.2016.03.018.

[16] Y. Wang, P. M. Rogers, C. Su, G. Varga, K. R. Stayrook, and T. P. Burris, “Regulation of cholesterologenesis by the oxysterol receptor, LXRα,” *J. Biol. Chem.*, vol. 283, no. 39, pp. 26332–26339, 2008, doi: 10.1074/jbc.M804808200.

[17] D. G. Thomas *et al.*, “LXR Suppresses Inflammatory Gene Expression and Neutrophil Migration through cis-Repression and Cholesterol Efflux,” *Cell Rep.*, vol. 25, no. 13, pp. 3774-3785.e4, 2018, doi: 10.1016/j.celrep.2018.11.100.

[18] N. Zelcer, C. Hong, R. Boyadjian, and P. Tontonoz, “LXR Regulates Cholesterol Uptake through Idol-dependent Ubiquitination of the LDL Receptor Noam,” *Science (80-.).*, vol. 325, no. 5936, pp. 100–104, 2009, doi: 10.1126/science.1168974.LXR.

[19] I. Paterniti *et al.*, “Liver X receptors activation, through TO901317 binding, reduces neuroinflammation in Parkinson’s disease,” *PLoS One*, vol. 12, no. 4, pp. 1–16, 2017, doi: 10.1371/journal.pone.0174470.

[20] C. H. Wu *et al.*, “Treatment with TO901317, a synthetic liver X receptor agonist, reduces brain damage and attenuates neuroinflammation in experimental intracerebral hemorrhage,” *J. Neuroinflammation*, vol. 13, no. 1, pp. 1–17, 2016, doi: 10.1186/s12974-016-0524-8.

[21] K. Mouzat *et al.*, “Regulation of brain cholesterol: What role do liver X receptors play in neurodegenerative diseases?,” *Int. J. Mol. Sci.*, vol. 20, no. 16, 2019, doi: 10.3390/ijms20163858.

[22] O. S. Kim, C. S. Lee, E. H. Joe, and I. Jou, “Oxidized low density lipoprotein suppresses lipopolysaccharide-induced inflammatory responses in microglia: Oxidative stress acts through control of inflammation,” *Biochem. Biophys. Res. Commun.*, vol. 342, no. 1, pp. 9–18, 2006, doi: 10.1016/j.bbrc.2006.01.107.

[23] J. R. Secor McVoy, A. A. Oughli, and U. Oh, “Liver X receptor-dependent inhibition of

microglial nitric oxide synthase 2," *J. Neuroinflammation*, vol. 12, no. 1, pp. 1–14, 2015, doi: 10.1186/s12974-015-0247-2.

[24] C. X. Zhang-Gandhi and P. D. Drew, "Liver X Receptor and Retinoid X Receptor Agonists Inhibit Inflammatory Responses of Microglia and Astrocytes," *J Neuroimmunol*, vol. 183, no. 1–2, pp. 50–59, 2007, [Online]. Available: https://www.ncbi.nlm.nih.gov/pmc/articles/PMC3624763/pdf/nihms412728.pdf.

[25] A. E. Frakes *et al.*, "Microglia induce motor neuron death via the classical NF-κB pathway in amyotrophic lateral sclerosis," *Neuron*, vol. 81, no. 5, pp. 1009–1023, 2014, doi: 10.1016/j.neuron.2014.01.013.Microglia.

[26] N. Kopitar-Jeraia, "Innate immune response in brain, nf-kappa b signaling and cystatins," *Front. Mol. Neurosci.*, vol. 8, no. DEC, pp. 1–9, 2015, doi: 10.3389/fnmol.2015.00073.

[27] X. Bi, J. Liu, Y. Yao, M. Baudry, and G. Lynch, "Deregulation of the phosphatidylinositol-3 kinase signaling cascade is associated with neurodegeneration in Npc1-/- mouse brain," *Am. J. Pathol.*, vol. 167, no. 4, pp. 1081–1092, 2005, doi: 10.1016/S0002-9440(10)61197-2.

[28] A. Oeckinghaus and S. Ghosh, "The NF-kappaB family of transcription factors and its regulation.," *Cold Spring Harb. Perspect. Biol.*, vol. 1, no. 4, pp. 1–14, 2009, doi: 10.1101/cshperspect.a000034.

[29] S. Ghisletti *et al.*, "Parallel SUMOylation-dependent pathways mediate gene- and signal-specific transrepression by LXRs and PPARγ," *Mol Cell*, vol. 25, no. 1, pp. 57–70, 2007, [Online]. Available: https://www.ncbi.nlm.nih.gov/pmc/articles/PMC3624763/pdf/nihms412728.pdf.

[30] E. C. Dresselhaus and M. K. Meffert, "Cellular specificity of NF-κB function in the nervous system," *Front. Immunol.*, vol. 10, no. MAY, 2019, doi: 10.3389/fimmu.2019.01043.

[31] K. Yamanaka, Y. Saito, T. Yamamori, Y. Urano, and N. Noguchi, "24(S)-hydroxycholesterol induces neuronal cell death through necroptosis, a form of programmed necrosis," *J. Biol. Chem.*, vol. 286, no. 28, pp. 24666–24673, 2011, doi: 10.1074/jbc.M111.236273.

[32] A. Meljon, Y. Wang, and W. J. Griffiths, "Oxysterols in the brain of the cholesterol 24-hydroxylase knockout mouse," *Biochem. Biophys. Res. Commun.*, vol. 446, no. 3, pp. 768–774, 2014, doi: 10.1016/j.bbrc.2014.01.153.

[33] S. Theofilopoulos *et al.*, "24(S),25-Epoxycholesterol and cholesterol 24S-hydroxylase (CYP46A1) overexpression promote midbrain dopaminergic neurogenesis in vivo," *J. Biol. Chem.*, vol. 294, no. 11, pp. 4169–4176, 2019, doi: 10.1074/jbc.RA118.005639.

[34] P. J. Crick *et al.*, “Formation and metabolism of oxysterols and cholestenoic acids found in the mouse circulation: Lessons learnt from deuterium-enrichment experiments and the CYP46A1 transgenic mouse,” *J. Steroid Biochem. Mol. Biol.*, vol. 195, no. September, 2019, doi: 10.1016/j.jsbmb.2019.105475.

[35] V. Leoni and C. Caccia, “Oxysterols as biomarkers in neurodegenerative diseases,” *Chem. Phys. Lipids*, vol. 164, no. 6, pp. 515–524, 2011, doi: 10.1016/j.chemphyslip.2011.04.002.

[36] H. Kölsch, R. Heun, A. Kerksiek, K. V. Bergmann, W. Maier, and D. Lütjohann, “Altered levels of plasma 24S- and 27-hydroxycholesterol in demented patients,” *Neurosci. Lett.*, vol. 368, no. 3, pp. 303–308, 2004, doi: 10.1016/j.neulet.2004.07.031.

[37] L. Bretillon *et al.*, “Plasma levels of 24S-hydroxycholesterol in patients with neurological diseases,” *Neurosci. Lett.*, vol. 293, no. 2, pp. 87–90, 2000, doi: 10.1016/S0304-3940(00)01466-X.

[38] V. Leoni, T. Masterman, P. Patel, S. Meaney, U. Diczfalusy, and I. Björkhem, “Side chain oxidized oxysterols in cerebrospinal fluid and the integrity of blood-brain and blood-cerebrospinal fluid barriers,” *J. Lipid Res.*, vol. 44, no. 4, pp. 793–799, 2003, doi: 10.1194/jlr.M200434-JLR200.

[39] G. Zuliani *et al.*, “Plasma 24S-hydroxycholesterol levels in elderly subjects with late onset Alzheimer’s disease or vascular dementia: A case-control study,” *BMC Neurol.*, vol. 11, no. 1, p. 121, 2011, doi: 10.1186/1471-2377-11-121.

[40] V. Leoni, T. Masterman, U. Diczfalusy, G. De Luca, J. Hillert, and I. Björkhem, “Changes in human plasma levels of the brain specific oxysterol 24S-hydroxycholesterol during progression of multiple sclerosis,” *Neurosci. Lett.*, vol. 331, no. 3, pp. 163–166, 2002, doi: 10.1016/S0304-3940(02)00887-X.

[41] A. Wuolikainen, J. Acimovic, A. LöVgren-Sandblom, P. Parini, P. M. Andersen, and I. BjöRkhem, “Cholesterol, oxysterol, triglyceride, and coenzyme q homeostasis in als. evidence against the hypothesis that elevated 27-hydroxycholesterol is a pathogenic factor,” *PLoS One*, vol. 9, no. 11, pp. 1–15, 2014, doi: 10.1371/journal.pone.0113619.

[42] F. D. Porter *et al.*, “Cholesterol oxidation products are sensitive and specific blood-based biomarkers for Niemann-Pick C1 disease,” vol. 2, no. 56, pp. 1–23, 2011, doi: 10.1126/scitranslmed.3001417.Cholesterol.

[43] M. Moutinho, M. J. Nunes, and E. Rodrigues, “Cholesterol 24-hydroxylase: Brain cholesterol metabolism and beyond,” *Biochim. Biophys. Acta - Mol. Cell Biol. Lipids*, vol. 1861, no. 12, pp. 1911–1920, 2016, doi: 10.1016/j.bbalip.2016.09.011.

[44] M. Moutinho *et al.*, “Neuronal cholesterol metabolism increases dendritic outgrowth and synaptic markers via a concerted action of GGTase-I and Trk,” *Sci. Rep.*, vol. 6, no.

January, pp. 1–18, 2016, doi: 10.1038/srep30928.

[45] M. A. Burlot *et al.*, “Cholesterol 24-hydroxylase defect is implicated in memory impairments associated with alzheimer-like Tau pathology,” *Hum. Mol. Genet.*, vol. 24, no. 21, pp. 5965–5976, 2015, doi: 10.1093/hmg/ddv268.

[46] E. Hudry *et al.*, “Adeno-associated virus gene therapy with cholesterol 24-hydroxylase reduces the amyloid pathology before or after the onset of amyloid plaques in mouse models of alzheimer’s disease,” *Mol. Ther.*, vol. 18, no. 1, pp. 44–53, 2010, doi: 10.1038/mt.2009.175.

[47] W. Cui, Y. Sun, Z. Wang, C. Xu, Y. Peng, and R. Li, “Liver X receptor activation attenuates inflammatory response and protects cholinergic neurons in APP/PS1 transgenic mice,” *Neuroscience*, vol. 210, pp. 200–210, 2012, doi: 10.1016/j.neuroscience.2012.02.047.

[48] L. Boussicault *et al.*, “CYP46A1, the rate-limiting enzyme for cholesterol degradation, is neuroprotective in Huntington’s disease,” *Brain*, vol. 139, no. 3, pp. 953–970, 2016, doi: 10.1093/brain/awv384.

[49] C. Nóbrega *et al.*, “Restoring brain cholesterol turnover improves autophagy and has therapeutic potential in mouse models of spinocerebellar ataxia,” *Acta Neuropathol.*, vol. 138, no. 5, pp. 837–858, 2019, doi: 10.1007/s00401-019-02019-7.

[50] N. Mast, M. A. White, I. Bjorkhem, E. F. Johnson, C. D. Stout, and I. A. Pikuleva, “Crystal structures of substrate-bound and substrate-free cytochrome P450 46A1, the principal cholesterol hydroxylase in the brain,” *Proc. Natl. Acad. Sci. U. S. A.*, vol. 105, no. 28, pp. 9546–9551, 2008, doi: 10.1073/pnas.0803717105.

[51] N. Mast, M. Linger, M. Clark, J. Wiseman, C. D. Stout, and I. A. Pikuleva, “In silico and intuitive predictions of CYP46A1 inhibition by marketed drugs with subsequent enzyme crystallization in complex with fluvoxamine,” *Mol. Pharmacol.*, vol. 82, no. 5, pp. 824–834, 2012, doi: 10.1124/mol.112.080424.

[52] M. Shafaati *et al.*, “The antifungal drug voriconazole is an effi cient inhibitor of brain cholesterol 24s-hydroxylase in vitro and in vivo,” *J. Lipid Res.*, vol. 51, no. 2, pp. 318–323, 2010, doi: 10.1194/jlr.M900174-JLR200.

[53] A. M. Petrov *et al.*, “CYP46A1 Activation by Efavirenz Leads to Behavioral Improvement without Significant Changes in Amyloid Plaque Load in the Brain of 5XFAD Mice,” *Neurotherapeutics*, vol. 16, no. 3, pp. 710–724, 2019, doi: 10.1007/s13311-019-00737-0.

[54] D. N. Mitroi *et al.*, “ NPC 1 enables cholesterol mobilization during long-term potentiation that can be restored in Niemann–Pick disease type C by CYP46A1 activation ,” *EMBO Rep.*, vol. 20, no. 11, pp. 1–18, 2019, doi: 10.15252/embr.201948143.

[55] A. Martín-Segura *et al.*, “Age-associated cholesterol reduction triggers brain insulin resistance by facilitating ligand-independent receptor activation and pathway desensitization,” *Aging Cell*, vol. 18, no. 3, 2019, doi: 10.1111/acel.12932.

[56] T. Nishi *et al.*, “Soticlestat, a novel cholesterol 24-hydroxylase inhibitor shows a therapeutic potential for neural hyperexcitation in mice,” *Sci. Rep.*, vol. 10, no. 1, pp. 1–10, 2020, doi: 10.1038/s41598-020-74036-6.

[57] Y. Urano, S. Ochiai, and N. Noguchi, “Suppression of amyloid-β production by 24S-hydroxycholesterol via inhibition of intracellular amyloid precursor protein trafficking,” *FASEB J.*, vol. 27, no. 10, pp. 4305–4315, 2013, doi: 10.1096/fj.13-231456.

[58] J. Brown *et al.*, “Differential expression of cholesterol hydroxylases in Alzheimer’s disease,” *J. Biol. Chem.*, vol. 279, no. 33, pp. 34674–34681, 2004, doi: 10.1074/jbc.M402324200.

[59] M. Patterson, “Niemann-Pick Disease Type C Summary Clinical Diagnosis,” pp. 1–21, 2019.

[60] R. J. Chandler *et al.*, “Systemic AAV9 gene therapy improves the lifespan of mice with Niemann-Pick disease, type C1,” *Hum. Mol. Genet.*, vol. 26, no. 1, pp. 52–64, 2017, doi: 10.1093/hmg/ddw367.

[61] C. Xie, X. M. Gong, J. Luo, B. L. Li, and B. L. Song, “AAV9-NPC1 significantly ameliorates Purkinje cell death and behavioral abnormalities in mouse NPC disease,” *J. Lipid Res.*, vol. 58, no. 3, pp. 512–518, 2017, doi: 10.1194/jlr.M071274.

[62] M. P. Hughes *et al.*, “AAV9 intracerebroventricular gene therapy improves lifespan, locomotor function and pathology in a mouse model of Niemann-Pick type C1 disease,” *Hum. Mol. Genet.*, vol. 27, no. 17, pp. 3079–3098, 2018, doi: 10.1093/hmg/ddy212.

[63] M. Praggastis *et al.*, “A murine Niemann-Pick C1 I1061T knock-In model recapitulates the pathological features of the most prevalent human disease allele,” *J. Neurosci.*, vol. 35, no. 21, pp. 8091–8106, 2015, doi: 10.1523/JNEUROSCI.4173-14.2015.

[64] N. Marschalek, F. Albert, V. Meske, and T. G. Ohm, “The natural history of cerebellar degeneration of Niemann-Pick C mice monitored in vitro,” *Neuropathol. Appl. Neurobiol.*, vol. 40, no. 7, pp. 933–945, 2014, doi: 10.1111/nan.12154.

[65] C. Xie, X. M. Gong, J. Luo, B. L. Li, and B. L. Song, “AAV9-NPC1 significantly ameliorates Purkinje cell death and behavioral abnormalities in mouse NPC disease,” *J. Lipid Res.*, vol. 58, no. 3, pp. 512–518, 2017, doi: 10.1194/jlr.M071274.

[66] J. E. Vance, “Transfer of cholesterol by the NPC team,” *Cell Metab.*, vol. 12, no. 2, pp. 105–106, 2010, doi: 10.1016/j.cmet.2010.07.004.

[67] M. T. Vanier and P. Latour, *Laboratory diagnosis of Niemann-Pick disease type C: The*

filipin staining test, vol. 126. Elsevier Ltd, 2015.

[68] R. Fu, N. M. Yanjanin, S. Bianconi, W. J. Pavan, and F. D. Porter, “Oxidative stress in Niemann-Pick disease, type C,” *Mol. Genet. Metab.*, vol. 101, no. 2–3, pp. 214–218, 2010, doi: 10.1016/j.ymgme.2010.06.018.

[69] D. Maetzel *et al.*, “Genetic and chemical correction of cholesterol accumulation and impaired autophagy in hepatic and neural cells derived from niemann-pick type C patient-specific iPS cells,” *Stem Cell Reports*, vol. 2, no. 6, pp. 866–880, 2014, doi: 10.1016/j.stemcr.2014.03.014.

[70] S. Sarkar *et al.*, “Impaired autophagy in the lipid-storage disorder niemann-pick type c1 disease,” *Cell Rep.*, vol. 5, no. 5, pp. 1302–1315, 2013, doi:10.1016/j.celrep.2013.10.042.

[71] S. M. Cologna *et al.*, “Human and Mouse Neuroinflammation Markers in Niemann-Pick Disease, type C1,” *J Inherit Metab Dis*, vol. 37, no. 1, pp. 1–18, 2014, doi: 10.1016/j.earlhumdev.2006.05.022.

[72] M. Walterfang *et al.*, “Imaging of neuroinflammation in adult Niemann-Pick type C disease: A cross-sectional study,” *Neurology*, vol. 94, no. 16, pp. E1716–E1725, 2020, doi: 10.1212/WNL.0000000000009287.

[73] A. Cougnoux *et al.*, “Microglia activation in Niemann-Pick disease, type C1 is amendable to therapeutic intervention,” *Hum. Mol. Genet.*, vol. 27, no. 12, pp. 2076–2089, 2018, doi: 10.1093/hmg/ddy112.

[74] H. M. Gao, H. Zhou, F. Zhang, B. C. Wilson, W. Kam, and J. S. Hong, “HMGB1 acts on microglia Mac1 to mediate chronic neuroinflammation that drives progressive neurodegeneration,” *J. Neurosci.*, vol. 31, no. 3, pp. 1081–1092, 2011, doi: 10.1523/JNEUROSCI.3732-10.2011.

[75] G. Srikrishna and H. H. Freeze, “Endogenous damage-associated molecular pattern molecules at the crossroads of inflammation and cancer,” *Neoplasia*, vol. 11, no. 7, pp. 615–628, 2009, doi: 10.1593/neo.09284.

[76] K. Hensley, “Neuroinflammation in AD:-mechanism, pathologic consequences, and potential for therapeutic manipulation,” *J. Alzheimers Dis.*, vol. 21, no. 1, pp. 1–14, 2010, doi: 10.3233/JAD-2010-1414.Neuroinflammation.

[77] B. Liu, S. D. Turley, D. K. Burns, A. M. Miller, J. J. Repa, and J. M. Dietschy, “Reversal of defective lysosomal transport in NPC disease ameliorates liver dysfunction and neurodegeneration in the npc1-/- mouse,” *Proc. Natl. Acad. Sci. U. S. A.*, vol. 106, no. 7, pp. 2377–2382, 2009, doi: 10.1073/pnas.0810895106.

[78] M. Maceyka, S. Milstien, and S. Spiegel, “The Potential of Histone Deacetylase Inhibitors

in Niemann–Pick Type C Disease," *FEBS J*, vol. 280, no. 24, pp. 1–9, 2013, doi: 10.1111/febs.12505.The.

[79] M. J. Nunes, M. Moutinho, M. J. Gama, C. M. P. Rodrigues, and E. Rodrigues, "Histone Deacetylase Inhibition Decreases Cholesterol Levels in Neuronal Cells by Modulating Key Genes in Cholesterol Synthesis, Uptake and Efflux," *PLoS One*, vol. 8, no. 1, 2013, doi: 10.1371/journal.pone.0053394.

[80] D. S. Ojala, D. P. Amara, and D. V. Schaffer, "Adeno-associated virus vectors and neurological gene therapy," *Neuroscientist*, vol. 21, no. 1, pp. 84–98, 2015, doi: 10.1177/1073858414521870.

[81] C. K. Fog and T. Kirkegaard, "Animal models for Niemann-Pick type C: implications for drug discovery & development," *Expert Opin. Drug Discov.*, vol. 14, no. 5, pp. 499–509, 2019, doi: 10.1080/17460441.2019.1588882.

[82] V. Pallottini and F. W. Pfrieger, "Understanding and treating niemann–pick type c disease: Models matter," *Int. J. Mol. Sci.*, vol. 21, no. 23, pp. 1–37, 2020, doi: 10.3390/ijms21238979.

[83] C. K. Fog and T. Kirkegaard, "Animal models for Niemann-Pick type C: implications for drug discovery & development," *Expert Opin. Drug Discov.*, vol. 14, no. 5, pp. 499–509, 2019, doi: 10.1080/17460441.2019.1588882.

[84] B. Karten, D. E. Vance, R. B. Campenot, and J. E. Vance, "Cholesterol accumulates in cell bodies, but is decreased in distal axons, of Niemann-Pick C1-deficient neurons," *J. Neurochem.*, vol. 83, no. 5, pp. 1154–1163, 2002, doi: 10.1046/j.1471-4159.2002.01220.x.

[85] C. M. Hawes, H. Wiemer, S. R. Krueger, and B. Karten, "Pre-synaptic defects of NPC1-deficient hippocampal neurons are not directly related to plasma membrane cholesterol," *J. Neurochem.*, vol. 114, no. 1, pp. 311–322, 2010, doi: 10.1111/j.1471-4159.2010.06768.x.

[86] R. A. Maue *et al.*, "A novel mouse model of Niemann-Pick type C disease carrying a D1005G-Npc1 mutation comparable to commonly observed human mutations," *Hum. Mol. Genet.*, vol. 21, no. 4, pp. 730–750, 2012, doi: 10.1093/hmg/ddr505.

[87] W. D. Park *et al.*, "Identification of 58 novel mutations in Niemann-Pick disease type C: Correlation with biochemical phenotype and importance of PTC1-like domains in NPC1," *Hum. Mutat.*, vol. 22, no. 4, pp. 313–325, 2003, doi: 10.1002/humu.10255.

[88] M. T. Vanier, "Niemann-Pick disease type C," *Vanier Orphanet J. Rare Dis.*, vol. 5, p. 16, 2010, [Online]. Available: http://www.ojrd.com/content/5/1/16.

[89] D. Ebrahimi-Fakhari *et al.*, "Reduction of TMEM97 increases NPC1 protein levels and

restores cholesterol trafficking in Niemann-pick type C1 disease cells," *Hum. Mol. Genet.*, vol. 25, no. 16, pp. 3588–3599, 2016, doi: 10.1093/hmg/ddw204.

[90] M. E. Gelsthorpe *et al.*, "Niemann-Pick type C1 I1061T mutant encodes a functional protein that is selected for endoplasmic reticulum-associated degradation due to protein misfolding," *J. Biol. Chem.*, vol. 283, no. 13, pp. 8229–8236, 2008, doi: 10.1074/jbc.M708735200.

[91] M. Praggastis *et al.*, "A murine Niemann-Pick C1 I1061T knock-In model recapitulates the pathological features of the most prevalent human disease allele," *J. Neurosci.*, vol. 35, no. 21, pp. 8091–8106, 2015, doi: 10.1523/JNEUROSCI.4173-14.2015.

[92] A. E. S. Simões *et al.*, "Efficient recovery of proteins from multiple source samples after trizol® or trizol®LS RNA extraction and long-term storage," *BMC Genomics*, vol. 14, no. 1, 2013, doi: 10.1186/1471-2164-14-181.

[93] S. J. Langmade *et al.*, "Pregnane X receptor (PXR) activation: A mechanism for neuroprotection in a mouse model of Niemann-Pick C disease," *Proc. Natl. Acad. Sci. U. S. A.*, vol. 103, no. 37, pp. 13807–13812, 2006, doi: 10.1073/pnas.0606218103.

[94] M. Gómez-Grau *et al.*, "New murine Niemann-Pick type C models bearing a pseudoexon-generating mutation recapitulate the main neurobehavioural and molecular features of the disease," *Sci. Rep.*, vol. 7, no. January, pp. 1–16, 2017, doi: 10.1038/srep41931.

[95] Y. H. Hung *et al.*, "Neurological Dysfunction in Early Maturity of a Model for Niemann–Pick C1 Carrier Status," *Neurotherapeutics*, vol. 13, no. 3, pp. 614–622, 2016, doi: 10.1007/s13311-016-0427-5.

[96] E. R. Whitney, T. L. Kemper, M. L. Bauman, D. L. Rosene, and G. J. Blatt, "Cerebellar Purkinje cells are reduced in a subpopulation of autistic brains: A stereological experiment using calbindin-D28k," *Cerebellum*, vol. 7, no. 3, pp. 406–416, 2008, doi: 10.1007/s12311-008-0043-y.

[97] G. Liao *et al.*, "Cholesterol accumulation is associated with lysosomal dysfunction and autophagic stress in Npc1-/- mouse brain," *Am. J. Pathol.*, vol. 171, no. 3, pp. 962–975, 2007, doi: 10.2353/ajpath.2007.070052.

[98] M. J. Elrick and A. P. Lieberman, "Autophagic dysfunction in a lysosomal storage disorder due to impaired proteolysis," *Autophagy*, vol. 9, no. 2, pp. 234–235, 2013, doi: 10.4161/auto.22501.

[99] K. Ohgane, F. Karaki, K. Dodo, and Y. Hashimoto, "Discovery of oxysterol-derived pharmacological chaperones for NPC1: Implication for the existence of second sterol-binding site," *Chem. Biol.*, vol. 20, no. 3, pp. 391–402, 2013, doi: 10.1016/j.chembiol.2013.02.009.

[100] J. Davidson *et al.*, “2-Hydroxypropyl-β-cyclodextrin is the active component in a triple combination formulation for treatment of Niemann-Pick C1 disease,” *Biochim. Biophys. Acta - Mol. Cell Biol. Lipids*, vol. 1864, no. 10, pp. 1545–1561, 2019, doi: 10.1016/j.bbalip.2019.04.011.

[101] J. J. Repa *et al.*, “Liver X receptor activation enhances cholesterol loss from the brain, decreases neuroinflammation, and increases survival of the NPC1 mouse,” *J. Neurosci.*, vol. 27, no. 52, pp. 14470–14480, 2007, doi: 10.1523/JNEUROSCI.4823-07.2007.

[102] K. Frudd, T. Burgoyne, and J. R. Burgoyne, “Oxidation of Atg3 and Atg7 mediates inhibition of autophagy,” *Nat. Commun.*, vol. 9, no. 1, pp. 1–15, 2018, doi: 10.1038/s41467-017-02352-z.

[103] M. Moutinho *et al.*, “Cholesterol 24S-Hydroxylase Overexpression Inhibits the Liver X Receptor (LXR) Pathway by Activating Small Guanosine Triphosphate-Binding Proteins (sGTPases) in Neuronal Cells,” *Mol. Neurobiol.*, vol. 51, no. 3, pp. 1489–1503, 2015, doi: 10.1007/s12035-014-8828-0.

[104] N. Mizushima and T. Yoshimori, “How to interpret LC3 immunoblotting,” *Autophagy*, vol. 3, no. 6, pp. 542–545, 2007, doi: 10.4161/auto.4600.

[105] M. Zervas, K. L. Somers, M. A. Thrall, and S. U. Walkley, “Critical role for glycosphingolipids in Niemann-Pick disease type C,” *Curr. Biol.*, vol. 11, no. 16, pp. 1283–1287, 2001, doi: 10.1016/S0960-9822(01)00396-7.

[106] R. M. Ransohoff, “A polarizing question: Do M1 and M2 microglia exist,” *Nat. Neurosci.*, vol. 19, no. 8, pp. 987–991, 2016, doi: 10.1038/nn.4338.

[107] F. O. Martinez and S. Gordon, “The M1 and M2 paradigm of macrophage activation: Time for reassessment,” *F1000Prime Rep.*, vol. 6, no. March, pp. 1–13, 2014, doi: 10.12703/P6-13.

[108] M. L. Dubbelaar, L. Kracht, B. J. L. Eggen, and E. W. G. M. Boddeke, “The Kaleidoscope of Microglial Phenotypes,” *Front. Immunol.*, vol. 9, no. July, p. 1753, 2018, doi: 10.3389/fimmu.2018.01753.

[109] M. Shafaati *et al.*, “Enhanced production of 24S-hydroxycholesterol is not sufficient to drive liver X receptor target genes in vivo,” *J. Intern. Med.*, vol. 270, no. 4, pp. 377–387, 2011, doi: 10.1111/j.1365-2796.2011.02389.x.